

THE PREDICTED IMPACT OF ORGANIC COATINGS ON ISOPRENE DERIVED
SECONDARY ORGANIC AEROSOL FORMATION

Mutian Ma

A thesis submitted to the faculty of the University of North Carolina at Chapel Hill in partial fulfillment of the requirements for the degree of Master of Science in the Department of Environmental Sciences and Engineering in the Gillings School of Global Public Health.

Chapel Hill
2017

Approved by:

William Vizuete

Havala Pye

Jason Surratt

@2017
Mutian Ma
ALL RIGHTS RESERVED

ABSTRACT

Mutian Ma: The Predicted Impact of Organic Coatings on Isoprene Derived Secondary Organic Aerosol Formation
(Under the direction of William Vizueté)

Fine particulate matter ($PM_{2.5}$) is known to have an adverse impact on health and climate. Secondary organic aerosol (SOA) is a source of $PM_{2.5}$ and the multiphase reactions of isoprene epoxydiols (IEPOX) is an important reaction pathway. Current chemical transport models do not include the impact of organic coatings of aerosols on IEPOX-derived SOA formation. This work for the first time predicts coating impact on IEPOX-derived SOA formation with the new lab based kinetic data and a 0-Dimensional model that reduced 31% qSOA formation. It was found that Henry's law constant (H) increase 10-fold led to 8-fold increase in IEPOX-derived SOA concentration. Diffusion coefficient of organic coating (D_{org}) was also critical on predicting IEPOX-derived SOA formation. Studies relying on different approaches resulted in a range of D_{org} value from $10^9 m^2/s$ to $10^{14} m^2/s$ resulting 1-100% SOA reduction. Assumptions regarding the RH above which diffusivity limitations were negligible also affected the model SOA predictions.

TABLE OF CONTENTS

LIST OF TABLES.....	v
LIST OF FIGURES.....	vi
LIST OF ABBREVIATIONS.....	vii
LIST OF SYMBOLS.....	ix
CHAPTER I: INTRODUCTION.....	1
CHAPTER II: MATERIAL AND METHODS.....	5
2.1 Reactive Uptake Algorithm.....	5
2.2 Measurement Data.....	8
Organic Coating Diffusion Coefficient.....	8
Field Site Measurement.....	9
2.3 Model Data.....	10
2.4 Model Performance Evaluation.....	10
CHAPTER III: RESULTS.....	12
3.1 Model Sensitivity.....	14
3.2 Model Optimization.....	17
CHAPTER IV: DISCUSSION.....	19
APPENDIX A: ADDITIONAL TABLE AND FIGURES.....	29
APPENDIX B: 0-D MODEL CODES.....	32
REFERENCES.....	57

LIST OF TABLES

Table 1 Summary of parameters used in all 0-D model simulation runs.....	21
Table 2 The normalized mean bias (NMB) and normalized mean error (NME) for of 2-methyltetrols (tetrols), isoprene epoxydiols organosulfates (IEPOXOS) and total secondary organic aerosol (SOA).....	22

LIST OF FIGURES

Figure 1 Model SOA predictions versus filter measurements (A) for the full range of the concentration and (B) for the measurement concentration range from 0-0.5 $\mu\text{g}/\text{m}^3$	23
Figure 2 Percent bias compared to filter measurement (A) for the full range of the concentration and (B) for the measurement concentration range from 0-0.5 $\mu\text{g}/\text{m}^3$	24
Figure 3 Model species predictions versus filter measurement for (A) IEPOXOS and (B) tetrols	25
Figure 4 The percent reduction of predicted hourly γ as a function of RH	26
Figure 5 Total predicted SOA sensitivity runs versus filter measurement for (A) coat and newH, and (B)) apD _{org} , Song, newH _{org} , 25p and 5p	27
Figure 6 Total predicted SOA from optimization run versus filter measurement (A) for the full range of the concentration and (B) for the measurement concentration range from 0-0.5 $\mu\text{g}/\text{m}^3$	28

LIST OF ABBREVIATIONS

PM _{2.5}	Particulate matter
POA	Primary Organic Aerosol
SOA	Secondary Organic Aerosol
VOC	Volatile Organic Compound
BVOC	Biogenic Volatile Organic Compound
C ₅ H ₈	Isoprene, 2-methyl-1,3-butadiene
NO _x	Nitrogen oxides
RH	Relative Humidity
OH	Hydroxyl Radical
ISOPOOH	Isoprene Hydroxyl Hydroperoxide
IEPOX	Isoprene Epoxydiols
SAPRC07	Statewide Air Pollution Research Center 07
CMAQ	Community Multiscale Air Quality Model
Tetrols	2-methyltetrols
2-MG	2-methylglyceric Acid
OS	Sulfate Ester Derivatives
AS	Ammonium Sulfate
ABS	Ammonium Bisulfate
PEG	Polyethylene Glycol
O:C	Oxygen-to-Carbon
0-D	0-dimension
SOAS	South Oxidant Aerosol Study

IEPOXOS	Isoprene Epoxydiols Organosulfates
γ	Reactive Uptake Coefficient
LWC	Liquid Water Content
PAM	Potential Aerosol Mass
HR-ToF-CIMS	High-resolution Time-of-flight Chemical Ionization Mass Spectrometer
LRK	Look Rock site, Tennessee, USA
SO _x	Sulfate Oxides
GC/EI-MS	Gas Chromatography Interfaced to an Electron Impact-mass Spectrometer
UPLC/DAD-ESI-HR-QTOFMS	High-resolution Quadrupole Time-of-flight Electrospray Ionization Mass Spectrometry
NMB	Normalized Mean Bias
NME	Normalized Mean Error

LIST OF SYMBOLS

$IEPOX_{(g)}$	IEPOX Gas Phase Concentration ($\mu g/cm^3$)
$IEPOXSOA_{(aerosol)}$	IEPOX-derived SOA Concentration ($\mu g/cm^3$)
SA	Surface Area ($\mu m^2/cm^3$)
v	IEPOX Gas Mean Molecular Speed (m/s)
r_p	Effective Molecular Particle Radius (cm)
D_g	IEPOX diffusivity in the gas phase (cm^2/s)
MW	Molecular Weight of IEPOX (g/mol)
α	Accommodation Coefficient
H	Henry's Law Coefficient (M/atm)
R	Gas Constant ($L * atm/(K * mol)$)
T	Temperature (K)
D_a	IEPOX Diffusivity in the Aerosol Phase (cm^2/s)
$K_{particle}$	Pseudo-first Order Rate Constant (s^{-1})
H_{org}	Effective Henry's Law Constant for an Organic Coating (M/atm)
l_{org}	Organic Coating Thickness (m)
D_{org}	Organic Coating Diffusivity (cm^2/s)
v	Mean Molecular speed (m/s)
r_p	Aerosol Seed Radius (m)
r_{core}	Aerosol Inorganic Core Radius (m)

q	Diffuso-reactive Parameter
$k_{H^+,water} a_{H^+}$	Reactive parameter from ISORROPIA II
$k_{H^+O_4^-,water}$	Reactive parameter from ISORROPIA II
$k_{NH_4^+,water}$	Reactive parameter from ISORROPIA II
$k_{H^+,SO_4^{2-}} a_{H^+}$	Reactive parameter from ISORROPIA II
$[HSO_4^-]$	Bisulfate Ion Concentration (mol/L)
$[NH_4^+]$	Ammonium Ion Concentration (mol/L)
$[SO_4^{2-}]$	Sulfate Ion Concentration (mol/L)
β	Speciation conversion rate
N_a	Avogadro's Number
η	Particle Viscosity ($Pa \cdot s$)
a	Gas Particle Radius (m)

CHAPTER I: INTRODUCTION

Fine particulate matter (PM_{2.5}), particulate matter with a diameter 2.5 μm or less, is known to have an adverse impact on health and climate¹. Forty-five percent of the global PM_{2.5} consists of organic materials that can be directly emitted as primary organic aerosols (POA) or is formed in the atmosphere as secondary organic aerosols (SOA)². SOA is formed via atmospheric chemical processes that rely on reactions of gas phase volatile organic compounds (VOCs) that are emitted into the atmosphere. A large emission source of VOCs into the atmosphere, and an important SOA precursor, are biogenic volatile organic compounds (BVOCs)³. There are many different types of BVOCs being emitted, but the largest global source is isoprene (2-methyl-1,3-butadiene, C₅H₈)⁴ and it is reported by Guenther et al.⁵ to have estimated emission of 500 to 750 Tg yr⁻¹.

Isoprene and its influence on SOA formation have been the focus of recent studies that have discovered increases of PM_{2.5} via a low nitrogen oxides (NO_x) multiphase pathway. It is now known that this pathway is influenced by aerosol seed acidity, ambient relative humidity (RH), and sulfate availability^{4, 6-26}. Under limited NO_x conditions, isoprene first reacts with hydroxyl radical (OH) to form first generation isoprene oxidation products such as isoprene hydroxyl hydroperoxide (ISOPOOH)²⁷. ISOPOOH can then further react with OH to form isoprene epoxydiols (IEPOX) which can partition onto pre-existing aerosol seed and produce IEPOX-derived SOA. IEPOX-derived SOA formation is affected by several physical and chemical parameters

including relative humidity, diffusion hindrances with an organic coating, particle reactivity, and the ability of aerosol seeds to absorb mass¹⁸⁻²⁰. Aerosol acidity can also enhance IEPOX-derived SOA formation²¹. As a result, the IEPOX reactive uptake process amidst high RH conditions with acidified inorganic aerosol seed is considered the main IEPOX-derived SOA reaction pathway in the atmosphere¹⁰. IEPOX-derived SOA will then undergo further reactions with or within aerosols to increase PM2.5 mass.

The IEPOX related oxidation products and reaction pathways are important and need to be included in models for accurate prediction and regulatory purposes. Gas phase reactions for IEPOX were introduced in the Statewide Air Pollution Research Center 07 (SAPRC07tic)^{28, 29} mechanism. This version of the mechanism introduced new IEPOX SOA species along with corresponding reaction rate constants³⁰. This mechanism was then implemented in the Community Multiscale Air Quality Model (CMAQ 5.1) permitting the prediction of isoprene derived SOA precursor. To predict SOA formation from these precursors additional particle phase reactions were added to the aerosol module via a heterogeneous reaction parametrization^{18, 28}. Using this new parameterization, CMAQ could predict the location of observed peaks in the Southeast US for the following isoprene derived SOA tracers¹⁸⁻²⁰: 2-methyltetrols (tetrols), 2-methylglyceric acid (2-MG) and sulfate ester derivatives (organosulfate, OS). The new heterogeneous pathway predicted tetrols and 2-MG were more consistent against the measurement yet OS were still significantly under predicted. This heterogeneous reactive uptake pathway provides a framework for this important pathway for isoprene SOA prediction, but uncertainty exists on many of its parameters. Furthermore, this implementation assumes that the pre-existing aerosol seeds are in a homogeneous

phase, only contain inorganic components, and that the organic constituents have no impact on the reactive uptake process.

In the CMAQ model, the process of IEPOX partitioning on to aerosol is treated as a homogeneous phase reaction with reactive parameters derived from empirical data. While in the real atmosphere, aerosol can be coated by organic layers formed by gas phase VOCs that will change the physical and chemical properties of the aerosol. A study by Zhang et al.³¹ used a flow tube reactor to generate α -pinene derived organic aerosol and used what observational data to estimate viscosity. The results found that α -pinene derived SOA had $\sim 10^8$ times higher viscosity than compared to water. Based on the Stokes-Einstein equation³², the α -pinene derived SOA diffusion coefficient is inversely proportional to the particle viscosity. Therefore, the organic diffusion coefficient should be reduced compared to pure inorganic diffusion impacting the organic coating diffusivity and hindering SOA formation. Riva et al.²¹ also used α -pinene derived oxidation product, but unlike Zhang, these researches formed an organic coating on ammonium sulfate (AS) and ammonium bisulfate (ABS) aerosol seeds. The IEPOX reactive uptake rates in these experiments were found to be reduced by up to 80% under a $\sim 50\%$ RH condition. Additional experiments with other organic coatings also found comparable results. Gaston et al.³³ found that Polyethylene glycol (PEG) derived coatings on the AS and ABS seeds reduced the IEPOX reactive uptake under 3 different RH condition and the reactive update was further reduced from 0.08 to less than 0.01 with higher PEG mass fraction.

The CMAQ implementation assumes a homogenous phase, however, in the atmosphere this may not be the case. The study of Song et al.³⁴ using optical

microscope observing droplets formed with various oxygen-to-carbon (O:C) indicated that aerosol droplet can have phase separation occurring under low O:C ratio (O:C<0.56) at low RH (<50%) and for test species with high O:C ratio (>0.8), phase separation never occurred. Pye et al¹⁹ predicted that over the continental US that organic and inorganic constituents within the aerosols are phase separated over 70% of the time. This phase separation has the potential to hinder SOA formation and hence influence model predictions.

A more accurate IEPOX-derived SOA model representation could be achieved by addressing the impacts of organic coatings and phase separation in heterogeneous reactive uptake algorithms. New chamber experimental data are now available allowing some constrains on critical parameters needed to simulate the changes in aerosol seed uptake due to coating type and under various RH conditions³⁵. This work developed a 0-dimension (0-D) box model incorporating the latest kinetic data that accounts for coating influences. Model inputs are constrained using measurement data from the 2013 South Oxidant Aerosol Study (SOAS). SOAS also provided particle phase filter measurement data of isoprene epoxydiols organosulfates (IEPOXOS) and tetrols that is used for a model performance evaluation.

CHAPTER II: MATERIAL AND METHOD

2.1 Reactive Uptake Algorithm

The formation of IEPOX-derived SOA is modeled in this work as a first order heterogeneous uptake reaction^{18-20, 36}:



In this first order heterogeneous reaction, rate constant k_{het} is defined as

$$k_{het} = \frac{SA}{\frac{r_p}{D_g} + \frac{4}{\nu\gamma}} \quad (2)$$

where SA is the aerosol surface area ($\mu\text{m}^2/\text{cm}^3$), ν is the mean molecular speed (m/s) in the gas phase, r_p is the effective molecular particle radius (cm), D_g is IEPOX diffusivity in the gas phase, MW is the molecular weight of IEPOX (g/mol), and γ is the reactive uptake coefficient.

For all simulation runs, the measured gas phase IEPOX concentration and temperature were provided for every 30 minutes as the input and the SA and r_p terms were calculated based on measurement dry mass¹⁶. D_g ($1.9 * (MW)^{-\frac{2}{3}}$) was taken from Schnoor³⁷ and Nguyen et al¹⁴, and ν was estimated by root mean square speed³⁷.

The heterogeneous reaction is parametrized using a reactive uptake coefficient (γ) that assumes a core-shell morphology. Song et al³⁸ used Raman microscopy to show the core-shell morphology from the mixtures of ammonium sulfate with

C5-dicarboxylic acids (glutaric, methylsuccinic, and dimethylmalonic acid), ammonium sulfate with C6-dicarboxylic acids (2-methylglutaric, 3-methylglutaric, and 2,2-dimethylsuccinic acid), and ammonium sulfate with C7-dicarboxylic acids (3-methyladipic acid, 3,3-dimethylglutaric acid and diethylmalonic acid). Zhang et al.³⁵ used scanning electron microscopy and atomic force microscopy methods to show the core-shell morphology of laboratory generated α -Pinene derived SOA coated aerosol. This core-shell morphology assumption were also made by Anttila et al.³⁹ and Gaston et al.⁴⁰ to update the resistor model with a coating term. These data suggest continuing to assume a core shell approach in this reactive uptake coefficient. The reactive uptake coefficient used in this study is defined in equation 3^{18-20, 36}

$$\frac{1}{\gamma} = \frac{1}{\alpha} + \frac{v}{4H * R * T * \sqrt{D_a * k_{particle}}} \frac{1}{\coth(q) - \frac{1}{q}} + \frac{v * l_{org} * r_p}{4 * H_{org} * R * T * D_{org} * r_{core}} \quad (3)$$

where α is the accommodation coefficient, H is the Henry's Law coefficient (M/atm), R is the gas constant ($L * atm / (K * mol)$), T is temperature (K), D_a is the IEPOX diffusivity in the aerosol core (cm^2/s^{-1}), and $k_{particle}$ is the pseudo-first order rate constant (s^{-1}), H_{org} (M/atm) is the effective Henry's Law constant for an organic coating and l_{org} is the organic coating thickness (m), D_{org} is the organic coating diffusivity (cm^2/s^{-1}), v is the mean molecular speed (m/s), r_p is the aerosol seed radius (m), and r_{core} is the aerosol inorganic core radius (m). In equation 3 q is the diffuso-reactive parameter defined in equation 4^{18-20, 36}

$$q = (r_p \sqrt{\frac{k_{particle}}{D_a}}) \quad (4)$$

An α of 0.2⁴¹ and H of 3.0e7 M/atm^{18-20, 28, 33, 40} were assumed to match the values used in CMAQ v5.2¹⁸⁻²⁰. A H_{org} value of 0.3 M/atm was used reported by Gaston et al.^{33, 40}. l_{org} has not been measured thus an initial estimation of coating thickness was made as 10% of total aerosol seed radius as shown in equation 5

$$l_{org} = 0.1 * r_p \quad (5)$$

r_{core} is defined in equation 6

$$r_{core} = r_p - l_{org} \quad (6)$$

This study uses a D_{org} relationship with RH that was based on the potential phase separation⁴² and is defined in equation 7^{31, 43}. The data provided by Zhang et al³¹ was obtained from experiments with a RH range of 15% to 70%. In this study an extrapolation of the diffusion coefficient was used for RH less than 15% and when RH is greater than 70% D_{org} is assumed to revert to the value of D_a .

$$D_{org} = e^{6.55 * RH - 34.49} \quad \text{when } RH < 70\%$$

$$D_{org} = D_a \quad \text{when } RH > 70\% \quad (7)$$

The $k_{particle}$ for IEPOX will be calculated assuming protonation of the IEPOX and nucleophilic addition as defined in equation 8. The ISORROPIA II⁴⁴ model used measured liquid water content (LWC) to calculate the parameters needed for $k_{particle}$ ²⁰

$$k_{particle} = k_{H^+,water} a_{H^+} LWC + k_{H^+O_4^-,water} [HSO_4^-] LWC + k_{NH_4^+,water} [NH_4^+] LWC + k_{H^+,SO_4^{2-}} a_{H^+} [SO_4^{2-}] \quad (8)$$

Equation 9 is used to define speciation between 2 different IEPOX SOA products, IEPOXOS and tetrols, based on the relative rates of precursor conversion.

$$IEPOXSOA = \beta * IEPOXOS + (1 - \beta) * tetrols \quad (9)$$

This conversion rate β is defined by the fraction of sulfate converted per total $k_{particle}$ shown in equation 10,

$$\beta = \frac{k_{H^+,SO_4^{2-}} - a_{H^+}[SO_4^{2-}]}{k_{particle}} \quad (10)$$

2.2 Measurement Data

Organic Coating Diffusion Coefficient

The estimation of the diffusion coefficient of IEPOX in the organic coating (D_{org}) were based on two indoor flow tube studies by Shrestha et al.⁴⁵ and Zhang et al.³¹. In these studies SOA was produced in a flow tube reactor with or without BVOC derived coatings. α -pinene was used to generate one coating layer at different concentrations under several RH levels. The Stokes-Einstein equation was then used to convert viscosity to diffusivity as shown in Equation 11³¹

$$D_{org} = \frac{RT}{N_A} * \frac{1}{6\pi\eta a} \quad (11)$$

where R is the gas constant (0.0821 L atm K⁻¹ mol⁻¹), T is the ambient temperature (K), N_A is Avogadro's number (6.022 * 10²³), η is the particle viscosity (Pa · s), and a is the gas particle radius (m).

A second study estimated D_{org} via reactive uptake measurements base on the experiments from Zhang et al.³⁵. Briefly described, a potential aerosol mass (PAM) reactor was coupled together with an atomizer to generate SOA coated inorganic acidic

particles. These particles were conditioned at selected relative humidity (RH) and then injected to a flow tube reactor to react with IEPOX at different time scales. The reactive uptake coefficient, γ , was determined by measuring the gas phase IEPOX concentration via an iodide-adduct high-resolution time-of-flight chemical ionization mass spectrometer (HR-ToF-CIMS, Aerodyne Research, Inc). By calculating γ_{IEPOX} from selected coating thicknesses, a resistor model was applied to derive the value of $H_{\text{org}}*D_{\text{org}}^{40}$ at the RH where the experiments were conducted. Varying the RH of the air where the particles were exposed to, each $H_{\text{org}}*D_{\text{org}}$ value at selected RH was calculated.

Field Site Measurements

Field measurements at the Look Rock, Tennessee (LRK) ground site during the SOAS field campaign provided inputs for the model simulations and IEPOX SOA tracer concentrations needed for the model evaluation. Ambient temperature, RH, and aerosol concentrations were obtained from measurements described in Budisulistiorini et al¹⁶. IEPOX and ISOPOOH were detected as the $[\text{CH}_3\text{COO}\cdot\text{C}_5\text{H}_{10}\text{O}_3]^-$ ion at m/z 177 by the Aerodyne high-resolution time-of-flight chemical ionization mass spectrometry (HR-ToF-CIMS) described in Budisulistiorini et al²⁰. The $\text{PM}_{2.5}$ samples were collected every 3 hours during the high-NO_x and sulfate oxides (SO_x) periods (intensive sampling periods), and every 11 hours during the low-NO_x and SO_x periods (regular sampling periods)¹⁶. Two punches were extracted per filter and one punch was used for analysis by gas chromatography interfaced to an electron impact-mass spectrometer (GC/EI-MS) and the other one was used for ultra-performance liquid chromatography coupled to both diode array detection and high-resolution quadrupole time-of-flight electrospray

ionization mass spectrometry (UPLC/DAD-ESI-HR-QTOFMS).

Tetrol concentrations were analyzed by GC/EI-MS (Hewlett-Packard (HP) 5890 Series II Gas Chromatograph equipped coupled to an HP 5971A Mass Selective Detector) and were quantified using authentic standards synthesized in-house¹⁶. IEPOXOS concentrations were analyzed by UPLC/DAD-ESI-HR-QTOFMS (Agilent 6500 series system equipped with a Waters Acquity UPLC HSS T3 column) and were quantified using an authentic standard synthesized in-house¹⁶.

2.3 Model Data

The equations described above were implemented in a 0-D model via Matlab software (version 2017a) to predict hourly average concentrations for tetrols and IEPOXOS. Based on previous work, a 6-hour model run was used to estimate the final concentration output of the tracer per input timestep^{15,20}. For example, to estimate the IEPOX SOA concentrations for 6 pm, a modeling run was initialized at 6 pm and only the final hour of that 6-hour run was used in the analysis. Then all the hourly output data were matched and averaged to compare with the 3-hour and 11-hour filter data¹⁶. All model runs were completed from 06/01/2013 to 07/15/2013 using SOAS 2013 field measurement at the LRK site as input for the model.

2.4 Model Performance Evaluation

Normalized mean bias (NMB) and normalized mean error (NME) were calculated for all runs. Normalized mean bias and normalized mean error were used for model evaluation as shown in equations 12 and 13.

$$NMB = \frac{\sum_1^N (Model - Obs)}{\sum_1^N (Obs)} * 100 \quad (12)$$

$$NMB = \frac{\sum_1^N |Model - Obs|}{\sum_1^N (Obs)} * 100 \quad (13)$$

where *Model* are the 0-D model predictions and *Obs* are the measurement data from the LRK site.

CHAPTER III: RESULTS

All model evaluations used hourly model predictions of total IEPOX-derived SOA from the 0-D model that were then averaged to match the 3 or 11-hour filters samples collected during SOAS at the LRK. The first simulation is the “base” run where IEPOX SOA formation was predicted by equation 4 without the third term, identical to the implementation in Budisulistiorini et al²⁰. In a second run, labelled “coat,” the full equation 4 with the coating term was used using the parameters described above and shown in Table 1. Figure 1 shows the correlation of predicted total IEPOX-derived SOA from the base run versus the measurements. As shown in figure 1 the correlation has a slope of 1.07, but the R^2 of 0.59 suggests a large variability. Table 2 provides the bias and error statistics and shows for the base run a NMB of -54.3% and a 67.5% NME. Most of predictions of total SOA were less than $0.7 \mu\text{g}/\text{m}^3$ with only less than 10% of the data points having higher concentrations with a peak of $1.8 \mu\text{g}/\text{m}^3$. Figure 2 shows the changes in bias and error across this concentration range. As shown in figure 2 the base run only over predicted 5 observed concentrations on average by 74% and under predicted all other measurements. As shown in figure 2 the under predicted bias increased linearly from 0% at $0.5 \mu\text{g}/\text{m}^3$ to 70% by $0.1 \mu\text{g}/\text{m}^3$ to nearly 100% at the lowest concentrations. The percent error showed a similar trend as shown in Appendix 1 figure S1. The prediction that had a bias of 140% was from a 11-hour filter that was collected from 06/09/2013 20:00 to 06/10/2013 07:00. The model predicted a constant

0.7 $\mu\text{g}/\text{m}^3$ SOA concentration for all 11 hours, while the field samples showed a measured concentration of 0.5 $\mu\text{g}/\text{m}^3$.

The addition of phase separation and organic coatings reduced the amount of IEPOX uptake and amount of SOA produced for every simulation. On average the coat run predicted 31% less total IEPOX-derived SOA when compared to predictions from the base run. Figure 1 shows the correlation of predicted total IEPOX-derived SOA for the coat run versus the measurements and the base run. The coat run predictions resulted in a decrease of the slope from the base run to 0.77 and a reduction of R^2 to 0.55. As shown in Table 2 the predictions from the coat run increased the NMB from -54.3% to -65.1% and increased the NME by 7.1%. Figure 2 shows correlation of total SOA percent bias versus model SOA concentrations. The coating term always reduced SOA formation increasing the negative bias from -61.4 to -74.9% for concentrations less than 0.5 $\mu\text{g}/\text{m}^3$. The bias was improved from 45.4% to 31.0% for the five filters that were over predicted.

The total predicted IEPOX-derived SOA was speciated into IEPOXOS and tetrols using equations 10 and 11. Figure 3 shows the correlation of the base and coat run predictions against filter measurements for individual tracers. The base run predicted slopes of 0.50 and 1.28 for IEPOXOS and tetrols. The under prediction of IEPOXOS and over prediction in tetrols resulted in a slope close to 1 for the total SOA correlation shown in figure 1. As shown in Table 2 the predictions of IEPOXOS from the base run had a NMB of -80.5% and for tetrols NMB of -28.6%. When coating effects were included the prediction of both IEPOXOS and tetrols were decreased for all model predictions there was an average 6.1% reduction for IEPOXOS and 15.5% reduction for

tetrols concentrations. This resulted in reducing the correlation slopes for IEPOXOS to 0.28 and tetrols to 1.05, R^2 were changed to 0.40 and 0.57. The reduction of the predicted overestimation of tetrols resulted in a better R^2 value. The greater decrease in tetrols is due to the relatively larger amount of $[HSO_4^-]$ and $[NH_4^+]$ ions versus sulfate ions leading to larger predictions of tetrols.

The model used in this study generated 792 hours of predicted IEPOX-derived SOA that were then averaged to match the 66 3 and 11-hour filters that were collected at the LRK site. Analysis of the pre-averaged hourly model data provides insights on the environmental conditions that were most impacted by the coatings effect. This data suggested that RH conditions had a notable change to γ . Figure 4 shows the average γ percentage reduction per 10% RH bin with N showing the number of hourly model predictions in each bin. For the coat run, the average γ reduction below the 70% RH cutoff were nearly 100% with the RH dependence and close to 0% above the 70% RH cutoff. Also shown in Figure 4 are the D_{org} values in cm^2/s . The 100% reduction in γ is largely the result of the magnitude of the assumed D_{org} value ($10^{-14} \frac{cm^2}{s}$) and the RH dependence only changes by 1 order of magnitude. For all model predictions with a RH of 70% the D_{org} is reduced by 9 orders of magnitude to $10^{-5} \frac{cm^2}{s}$ resulting in a negligible influence of coatings.

3.1 Model Sensitivity

The γ has several uncertainties including H, H_{org} , D_{org} , and I_{org} . All the uncertain variables were explored via model sensitivity runs. For this analysis, we focused on total SOA to mitigate the intrinsic uncertainties brought by the model speciation. Table 1 summarizes these sensitivity runs, where 1 coating parameter was modified. The newH

run addressed the uncertainty of Henry's law constant with a 10-fold H increase to $3e8 M/atm$, which is within the reported upper range found in the literature^{40, 46, 47}. The newH_{org} run increased H_{org} to a value of $3e7 M/atm$ as an upper bound test. The Song run uses a larger D_{org} value than the coat run converted from the viscosity of isoprene oxidation products generated from an oxidation flow reactor^{19, 42}. It is important to note that the D_{org} in the Song run assumes no RH cutoff. The apD_{org} run increases D_{org} value than the coat run based on experiments that used injected α -pinene oxidation products as a coating. In this work the authors assumed a D_{org} with an 80% RH cutoff³⁵. The 5p and 25p runs focused on the sensitivity of the thickness of the coating. In these simulations, a 5% or a 25% coating thickness was assumed in contrast to the 10% coating thickness assumed in the coat run.

Figure 5 shows the correlation of total modeled SOA versus observations for all sensitivity runs and the coat run. As shown in Figure 5, with a 10 times greater H , the newH run increased the correlation by more than 7 times compared with the IEPOX-derived SOA predicted in the coat run. When compared to the coat run the newH run produced the largest increases in model predicted SOA. The NMB increased from -38% to 223%. The increase in H_{org} in the newH_{org} run also produced increases relative to the coat run. As shown in Table 2 these increases resulted in model performance of the newH_{org} being similar to that of the base run. As the H_{org} and the D_{org} dictate gas phase IEPOX uptake onto the coating layer, the highest H_{org} used in the newH_{org} run made the coating layer behave like the aerosol core and stopped IEPOX gas uptake inhibition.

In all other sensitivity runs the changes in parameters resulted in lowering the predicted SOA when compared to the coat run. The lower D_{org} used in the apD_{org} run

compared to the coat run changed the correlation to 0.62 as shown in Figure 5. Table 2 shows that worsened NMB of -68.1%. The D_{org} increase in the Song run predicted the least amount of SOA concentration and reduced the slope to 0.22. The NMB was changed from -54.3% to -84.6%. As also shown Figure 5 the correlation predicted by modifying different coating thickness had relatively less impact on SOA when compared to predictions made in the coat run. Both increasing or decreasing the coating thickness changed the correlations less than 0.01.

Figure 4 also shows the γ reduction and D_{org} values for the ap D_{org} and Song runs against RH. The remaining runs can be found in figure S2. These γ reductions are driven by the change of D_{org} which is a function of RH. And the RH cutoff assumed minimal coating impact beyond the cutoff value also affected the γ predictions. Average D_{org} values are shown on the top of each column in figure 4. 3 RH range, <70%, 70-80%, 80-100%, were picked for analysis due to 3 different RH cutoff: 70% for the coat run, 80% for the ap D_{org} run, and no cutoff for the Song run.

When the RH is below 70%, the coat run has 99.9% γ reduction, the ap D_{org} run has 30% γ reduction, and the Song has 66% γ reduction dictated by the D_{org} in different magnitude where D_{org} for the coat run is 4 magnitudes smaller than the Song and 6 magnitudes smaller than the ap D_{org} run. When the RH is between 70-80%, the coat run has 0.3% γ reduction due to the 70% RH cutoff, the ap D_{org} run has 13% γ reduction, and the Song has 40% γ reduction where the D_{org} for the coat run is 2 magnitudes greater than the ap D_{org} run and 3 magnitudes greater than the Song run. When the RH is above 80%, the ap D_{org} runs reached the cutoff RH and predicted 0.3% γ reduction. The Song does not have a RH cutoff, therefore predicted 11% γ reduction.

With different RH cutoff for different D_{org} functions, the model performance were affected with varied γ . When the RH is between 70-80%, the coat, the ap D_{org} , and the Song run predicted -91%, -88%, and -93% NMB. When the RH is greater than 80%, the 3 runs predicted -74%, -74%, and -79% NMB. Changing RH cutoff from 70% to 80% improved model performance for 70-80% RH range but by removing RH cutoff worsened the model performance for 80-100% RH range.

3.2 Model optimization

To determine an optimized set of model parameters a total of 8 simulations, shown in table S1, were produced and compared against filter data with a goal of minimizing NMB and NME. As shown in Table 2 the NMB and NME for the opt8 run were improved to -26.2% and 66.6% and is the overall best run in all 8 optimization runs. In the opt8 run the parameters for the ap D_{org} was used with an increase of H from $3.0e7$ to $8.0e7$ M/atm . The opt8 run was able to increase lower concentration 700 times compared to the coat run. The significant increase was mainly contributed by the SOA formed under the 70-80% RH condition. Figure 6 shows the coat, base, and opt8 runs versus observations. The opt8 run had the best overall slope of 1.04 and R^2 of 0.60. No significant R^2 improvement was observed due to the under predictions at measurement $< 0.5 \mu g/m^3$ as shown in figure 6. The under prediction in this range was -24.7% NMB. For these lower predictions to match observations, an H value of $3e8$ M/atm , which is still within the highest reported H range from the literature⁴⁰ had to be used. Implementing this H value would over predict more than 8 times for the high concentrations. The opt4 run predicted the overall best NMB of -34.5% and NME of 69.7% followed by the opt8 run of 35.7% NMB and 71.3% NME. Yet the opt4 run

predicted 38.9% NMB at measurement $< 0.5 \mu\text{g}/\text{m}^3$, which consists 90% of the measurement data, compared to 24.7% NMB for the opt8 run. Hence the opt8 run is still predicts the best estimation for the 0-D model.

CHAPTER IV: DISCUSSION

The updated coating term in the reactive uptake algorithm affected IEPOX gas uptake by reducing 31% predicted SOA. The 0-D model shows the H parameter has the highest impact on model SOA prediction. A 10-fold increase in H to $3.0e8 \text{ M/atm}$ led to 8-fold increase in IEPOX-derived SOA concentration. This value is within the current literature reported H range from $2.7e6 \text{ M/atm}$ to $4.0e8 \text{ M/atm}$ ^{18-20, 33, 40, 46, 48}. D_{org} is reducing IEPOX-derived SOA formation and assumes electrolyte rich seeds¹⁹. When the D_{org} is $10^{14} \text{ m}^2/\text{s}$, IEPOX uptake is completely inhibited in the model while when the D_{org} is $10^9 \text{ m}^2/\text{s}$, IEPOX uptake is reduced by less than 1%. D_{org} was either converted from viscosity^{19, 31, 42, 49} or estimated with empirical data fitted with the resistor model from Gaston et al^{35, 40}. Different RH cutoff with corresponding D_{org} functions were able to affect the model performance with less than 10% for RH <70%, 70-80% and 80-100%. At least 40% γ reduction was predicted for RH <70%. In contrast, a maximum of 13% γ reduction was predicted for RH>70% within all sensitivity runs showing less significant RH impact on IEPOX-derived SOA formation at high RH. All model runs except for the newH run under predicted concentrations at the low end (*measurement* < $0.5 \mu\text{g}/\text{m}^3$).

With the updated resistor 0-D model and H of $8e7 \text{ M/atm}$, H_{org} of 0.3 M/atm , RH cutoff at 80%, D_{org} from α -pinene derived data³⁵, the model predicted more SOA concentration at the lower end yet still generated -43% NMB and -13% NMB for concentration greater than $0.5 \mu\text{g}/\text{m}^3$.

This work uses organic diffusion coefficient derived from α -pinene oxidant and only represents part of the organic coating constituents. Other constituents include anthropogenic and other biogenic sources could have a different impact on the uptake^{19, 46, 47, 50, 51}. D_{org} function is converted based on flow tube experiment data³⁵ under RH condition between 15-50% and empirical uptake calculation^{18, 40}. Further, ISORROPIA II²⁰ predicted $k_{particle}$ assuming a pure inorganic condition⁴⁴ leading to the uncertainty in these predictions. Further studies on constraining these parameters including H , D_{org} , and H_{org} in the resistor model and predicting more accurate $k_{particle}$ could help the model better predict IEPOX-derived SOA.

The under prediction of total SOA in $0-0.5 \mu g/m^3$ suggests H value used in the current CMAQ v5.2 ($3.0e7 M/atm$) should be higher. The updated resistor model suggests that the organic coating layer could have significant impact on the IEPOX-derived SOA formation and the potential to implement this resistor model in to regulatory model for IEPOX-derived SOA schematic update. RH is another important modulator of coating diffusion coefficient which directly affect γ .

The expansion of IEPOX heterogeneous reaction in CMAQ^{18, 48} helped better understand NOx and Sulfur control strategy and impact on $PM_{2.5}$ formation. The update of IEPOX coating resistor model in regulatory air quality model can provide a more accurate SOA formation pathway for IEPOX. Including organic coatings can change the impact by both anthropogenic and biogenic emission hence affect SOA control strategy and method for different regions.

Table 1. Summary of parameters used in all 0-D model simulation runs. H is the effective Henry's law coefficient for IEPOX partitioning onto inorganic aerosol, H_{org} is the effective Henry's law coefficient for IEPOX partitioning onto organic coating, RH is relative humidity, D_{org} is the IEPOX gas diffusion coefficient through organic coating, l_{org} is the thickness of coating layer, and R is the radius of aerosol seed.

Runs	H (M/atm)	H_{org} (M/atm)	RH cutoff	D_{org} (m/s ²) (RH<cutoff)	D_{org} (m/s ²) (RH>cutoff)	l_{org} (m)
base	3.00E+07	NA	NA	NA	NA	NA
coat	3.00E+07	0.3	70	$e^{(6.55 \cdot RH - 34.488)} \cdot 10^4$	1.00E-09	0.1 * R
newH	3.00E+08	0.3	70	$e^{(6.55 \cdot RH - 34.488)} \cdot 10^4$	1.00E-09	0.1 * R
newH _{org}	3.00E+07	3.0E+07	70	$e^{(6.55 \cdot RH - 34.488)} \cdot 10^4$	1.00E-09	0.1 * R
IsopD _{org}	3.00E+07	0.3	NA	$10^{(7.18 \cdot RH - 12.7)} \cdot 10^4$	1.00E-09	0.1 * R
apD _{org}	3.00E+07	0.3	80	$e^{(12.901 \cdot RH)} \cdot 2 \cdot 10^{-7}$	1.00E-09	0.1 * R
5p	3.00E+07	0.3	70	$e^{(6.55 \cdot RH - 34.488)} \cdot 10^4$	1.00E-09	0.05 * R
25p	3.00E+07	0.3	70	$e^{(6.55 \cdot RH - 34.488)} \cdot 10^4$	1.00E-09	0.25 * R
opt1	2.70E+06	0.3	80	$e^{(12.901 \cdot RH)} \cdot 10^{-7}$	1.00E-09	0.1 * R
opt2	3.00E+08	0.3	80	$e^{(12.901 \cdot RH)} \cdot 10^{-7}$	1.00E-09	0.1 * R
opt3	3.00E+08	0.3	NA	$10^{(7.18 \cdot RH - 12.7)} \cdot 10^4$	NA	0.1 * R
opt4	3.00E+08	0.3	NA	$10^{(7.18 \cdot RH - 12.7)} \cdot 10^4$	NA	0.05 * R
opt5	3.00E+08	0.3	80	$e^{(12.901 \cdot RH)} \cdot 10^{-7}$	1.00E-09	0.25 * R
opt6	1.00E+08	0.3	80	$e^{(12.901 \cdot RH)} \cdot 10^{-7}$	1.00E-09	0.1 * R
opt7	9.00E+07	0.3	80	$e^{(12.901 \cdot RH)} \cdot 10^{-7}$	1.00E-09	0.1 * R
opt8	8.00E+07	0.3	80	$e^{(12.901 \cdot RH)} \cdot 10^{-7}$	1.00E-09	0.1 * R

Table 2. The normalized mean bias (NMB) and normalized mean error (NME) for total secondary organic aerosol (SOA) with the difference compare to the base in parentheses. Run parameters are summarized in table 1.

Runs	NMB	NME
	Total SOA	Total SOA
base	-54.3	67.5
coat	-65.1 (-10.8)	74.6 (7.1)
newH _{org}	-54.4 (-0.1)	67.5 (0.0)
newH	178 (232)	248 (180)
IsopD _{org}	-84.6 (-30.3)	84.6 (17.1)
apD _{org}	-68.1 (-13.8)	72.6 (5.1)
5p	-64.7 (-10.4)	74.6 (7.1)
25p	-66.3 (-12.0)	74.6 (7.1)
opt8	-35.7 (18.6)	71.3 (3.8)

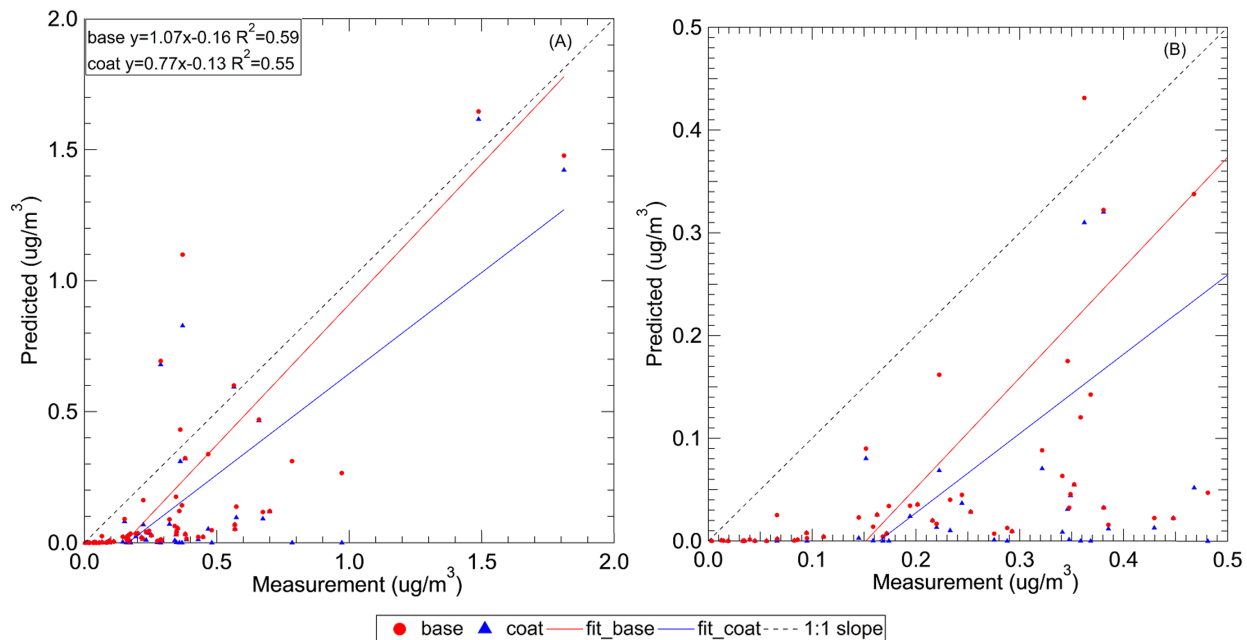


Figure 1. Model predictions of 45 days from the base (red circle) and coat (blue triangle) runs versus filter measurements collected at Look Rock site for total IEPOX-derived SOA for the (A) all data and (B) for concentration range from 0-0.5 $\mu\text{g}/\text{m}^3$.

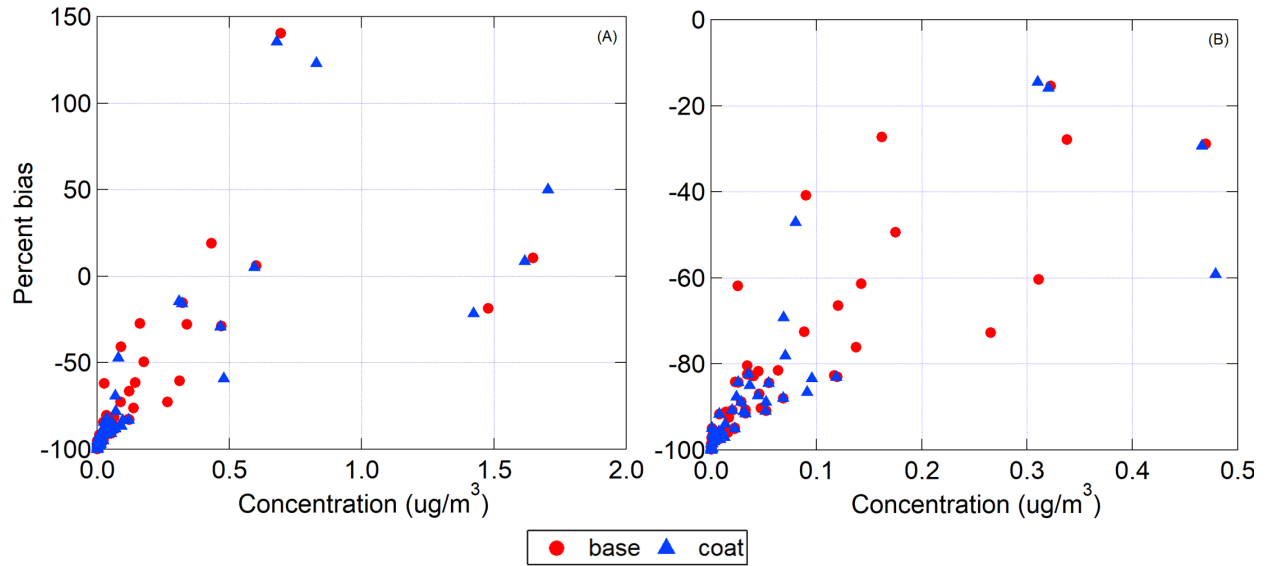


Figure 2. Percent bias of predicted compared to the filter measurements from Look Rock site for (A) across all predicted concentrations and (B) for concentration range from 0-0.5 $\mu\text{g}/\text{m}^3$ for the base (red circle) and coat (blue triangle) runs.

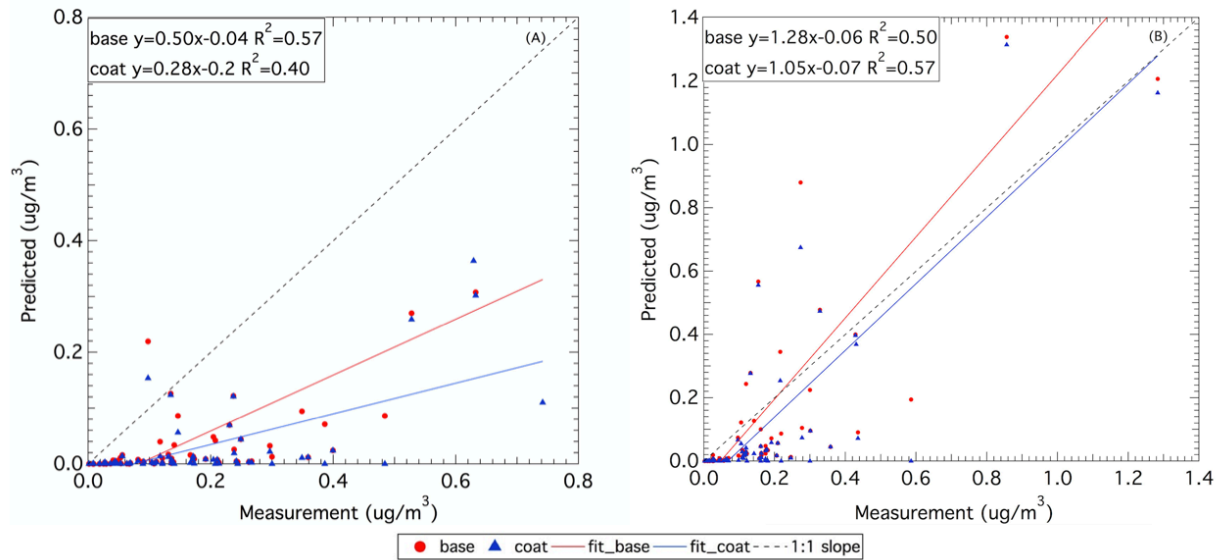


Figure 3. Model predictions from the base (red circle) and coat (blue triangle) runs versus filter measurements from Look Rock site for (A) the isoprene epoxydiols (IEPOX) derived SOA tracers of isoprene epoxydiols organosulfates (IEPOXOS) and (B) 2-methyltetrols (tetrols).

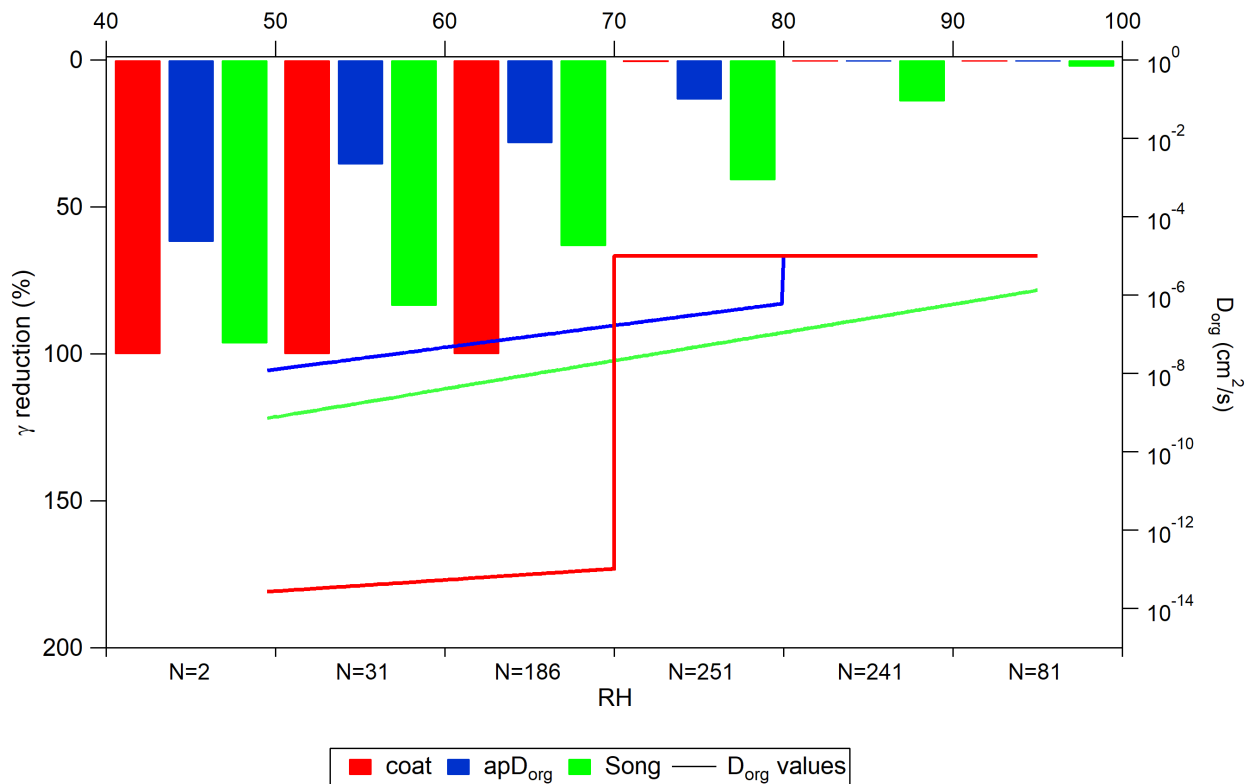


Figure 4. The percent reduction of predicted hourly γ and D_{org} values as a function of RH (10% bin). For the coat (red), apD_{org} (blue) and Song (green) runs, N is the number of hourly prediction points under corresponding RH bin. Lines with corresponding colors are D_{org} values ($\frac{\text{cm}^2}{\text{s}}$) calculated by RH. Model run parameters are summarized in table 1.

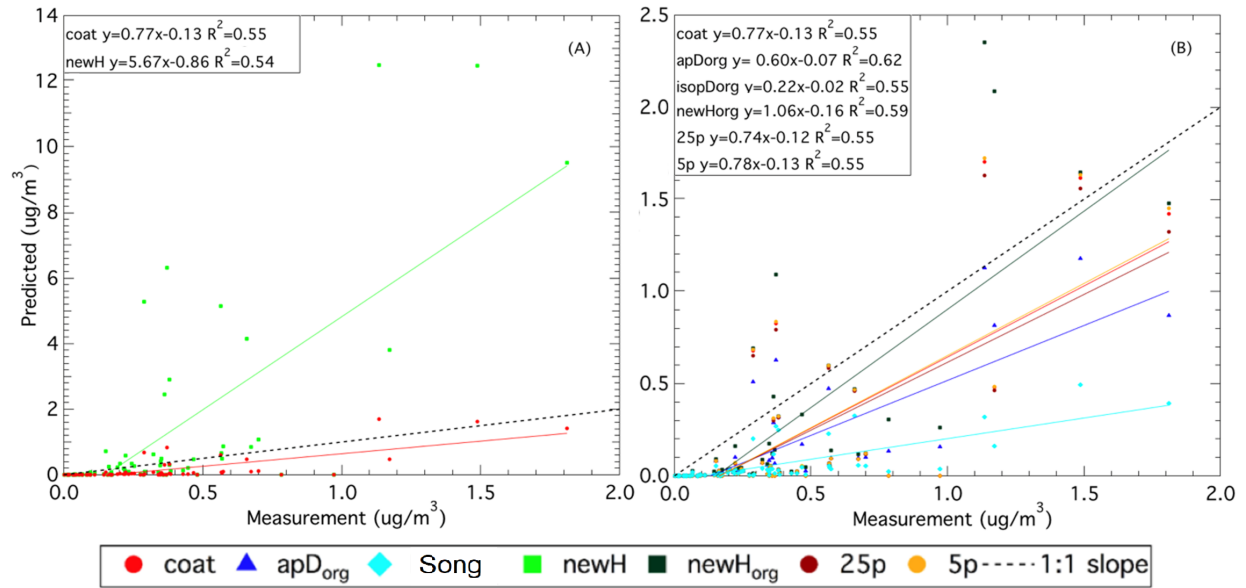


Figure 5. Total predicted SOA sensitivity runs versus measurement from Look Rock site for (A) coat (red circle), newH (light green square), and (B) apD_{org} (blue triangle), Song (teal diamond), newH_{org} (dark green square), 25p (brown circle) and 5p (yellow circle) runs. Model runs parameters are summarized in Table 1.

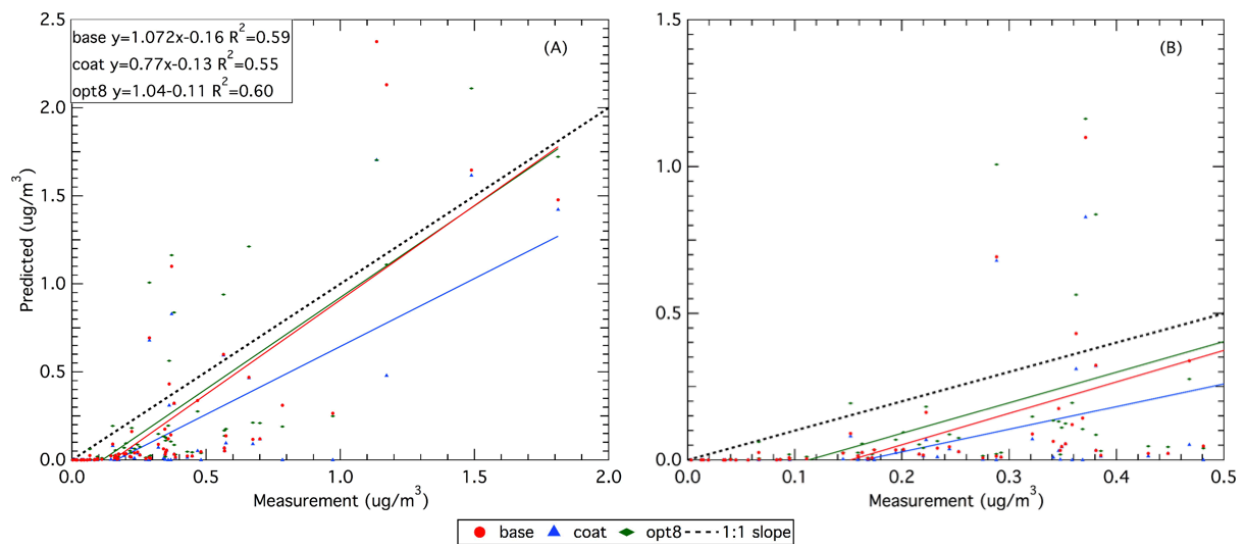


Figure 6. Total predicted SOA from optimization run versus filter measurement data Look Rock site with base (red circle), coat (blue triangle) and opt8 (green diamond) runs for (A) the full range of the concentration and (B) for the measurement concentration range from 0-0.5 $\mu\text{g}/\text{m}^3$.

APPENDIX A: ADDITIONAL TABLE AND FIGURES

Table S1. The normalized mean bias (NMB) and normalized mean error (NME) for total secondary organic aerosol (SOA) of the optimization runs with the difference compare to the base in parentheses. Run parameters are summarized in table 1.

Runs	Total SOA	
	NMB	NME
base	-38.8	69.7
opt1	-94.8 (-56)	94.8 (25.1)
opt2	51.9 (90.7)	108.7 (39.0)
opt3	-59.9 (-21.1)	72.7 (3.0)
opt4	-35.0 (3.8)	67.3 (-2.4)
opt5	-2.2 (36.6)	89.7 (20.0)
opt6	-18.8 (20)	70.3 (0.6)
opt7	-23.8 (15)	68.0 (-1.7)
opt8	-29.0 (9.8)	66.5 (-3.2)

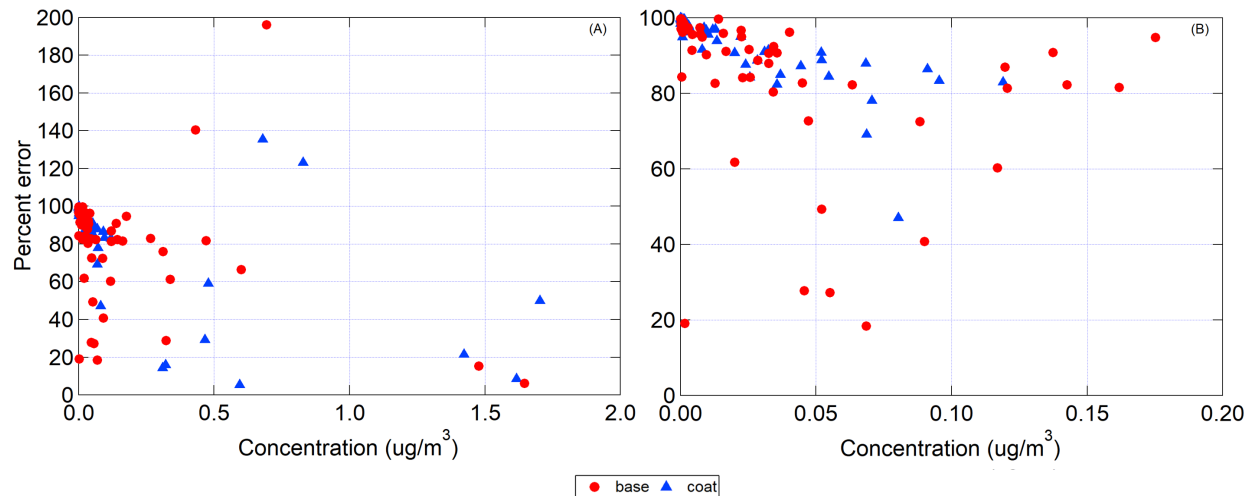


Figure S1. Percent bias of predicted compared to the filter measurements from Look Rock site for the base (red circle) and coat (blue triangle) runs.

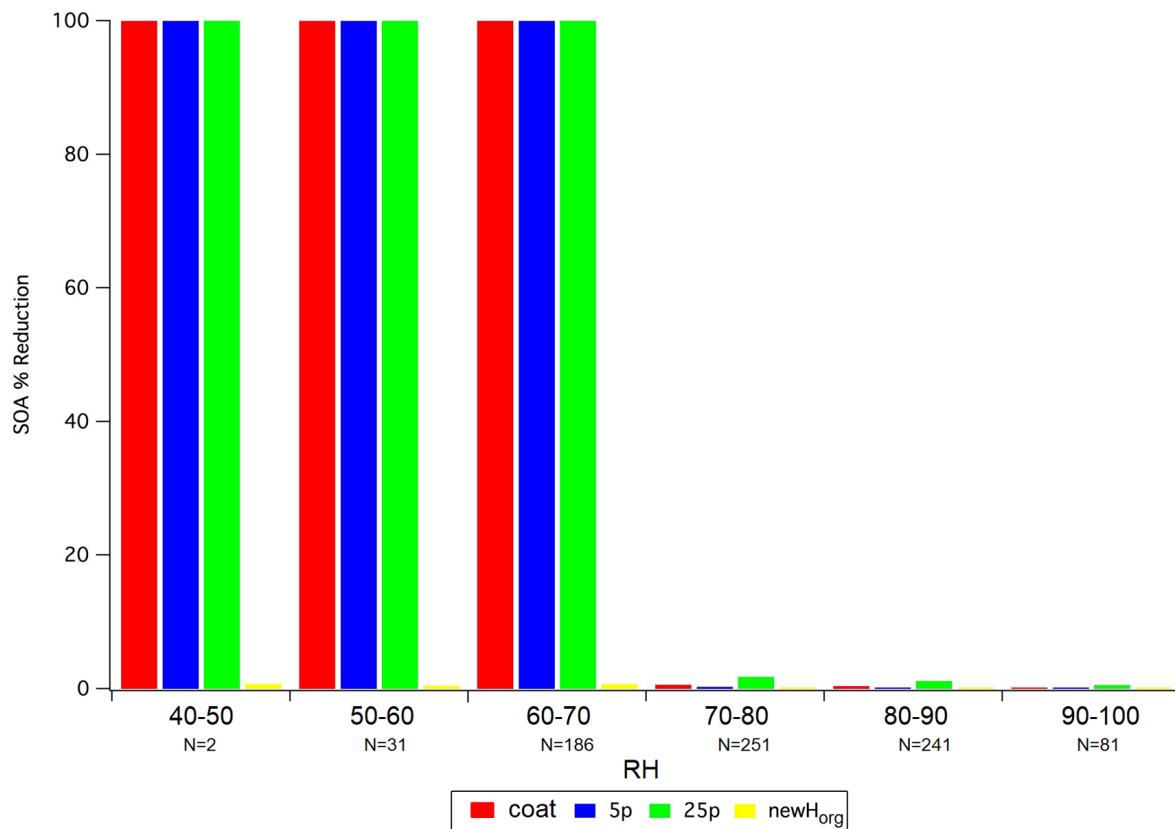


Figure S2. The percent reduction of hourly γ as a function of measured RH (10% bin). N is the number of hourly prediction points under corresponding RH bin. For the coat (red), 5p (blue), 25p (green), and newH_{org} runs, Model run parameters are summarized in table 2.

APPENDIX B: 0-D MODEL CODES

Cmaq_driver.m

% Main CMAQ uptake driving routine

% This routine interacts with the other files including inputs and separate functions

%%

% 9/17/14 SHB

% Added nested for loop

%%

% August 2015 HOTP

% Modified to include IEPOX conc calculation, similar kp formula for both CMAQ and simpleGAMMA,

% and BETA calculation for simpleGAMMA

%%

% 8/27/15 SHB

% Added kpout in routine to get kp values

%%

% 4/9/16 SHB

% Added parameter aRp for estimated radius of particle

%%

% 8/2016 HOTP

% Updated aRp, awL, and aSa for missing species (water, organics, water)

% added 3VdivSrp diagnostic which should be between 0.8 and 10,000 for valid points

%%

```

% 8/2016 SHB

% Added routine to save awL per line outside loop

% Added routine to save LWC, newSA

%=====

=====

clc;

close all;

clear;

% Importing Look Rock (LRK) data.

headerlinesIn = 1;

delimiterIn=',';

LRK = importdata('SOAS_LRK_iso6_rev2.csv',delimiterIn,headerlinesIn);

[m,n] = size(LRK.data);

% unit conversion factors

ugtog = 1e-6;

OAdensity = 1.4;           %g/cm3, Hallquist et al. 2009 in Budisulistiorini et al.

2016 ACP

m3tocm3 = 100^(-3);       %1m^3=100^3cm3

aerosoldensity = 1.5;     %g/cm3, avg aerosol density

```

inorgdensity = 1.7; %g/cm3, density of ammonium sulfate, ammonium
bisulfate

waterdensity = 1.0; %g/cm3, water density

% Computing uptake for LRK data

iepozos = [];

tetrol = [];

totsoa = [];

beta = [];

gma = [];

threeVdivSrp = [];

savenewawL = [];

kparticle = [];

iepox = [];

savenewLWC = [];

savenewSA = [];

savenewHplus = [];

pH = [];

lcoat = [];

for i=1:m

 runsuccess = false;

```

awL = LRK.data(i,2);           % cm3/cm3 air
aHplusActivity = LRK.data(i,3); % H+, mol/L aerosol
ay072 = LRK.data(i,4);         % HSO4, mol/L aerosol
ay073 = LRK.data(i,5);         % SO4, mol/L aerosol
awaterconc = LRK.data(i,6);    % H2O, mol/L aerosol
aIEP = iepox_fun( LRK.data(i,7), LRK.data(i,1) ); % inputs: aIEP, datetime
%aSa = LRK.data(i,8);          % particle surface area, cm2/cm3
aT = LRK.data(i,9);           % temperature, K
aRH = LRK.data(i,10);         % RH, fraction (0,1)
apH = LRK.data(i,11);         % pH
% not in original CMAQ version:
aNH4 = LRK.data(i,12);        % NH4, mol/L aerosol
%aRp = LRK.data(i,13);        % wet particle radius, cm (dry
radius converted by adding isorropia water)

% August 2016 updates: new quantities
org = LRK.data(i, 14);        % ug/m3 air, organics (ACSM)
water = LRK.data(i, 15);      % ug/m3 air, liquid water (ISORROPIAII)
Imass = LRK.data(i, 16);      % ug/m3 air, total ISORROPIA aerosol
mass (inorganic + water)
sadry = LRK.data(i, 17);      % cm2/cm3, dry aerosol surface area
(measured)

```

```

rpdry = LRK.data(i, 18);           % cm, dry partile radius (mode of size dist)

% correct aerosol volume for organics
actualvol = (org.*ugtog./OADensity.*m3tocm3+awL);   % add organics (w/ unit
conv) to particle volume, cm3 aerosol/cm3 air
aHplusActivity = aHplusActivity./actualvol.*awL;
ay072 = ay072./actualvol.*awL;
ay073 = ay073./actualvol.*awL;
awaterconc = awaterconc./actualvol.*awL;
aNH4 = aNH4./actualvol.*awL;
awL = actualvol;                   % add organics (w/ unit conv) to particle
volume, cm3 aerosol/cm3 air

% correct aerosol surface area for water. Measured Sa includes organics and
inorganics but not water. cm2/cm3
aSa =
sdry.*((Imass./inorgdensity+org./OADensity+water./waterdensity)./(Imass./inorgdensity
+org./OADensity))^(2.0/3.0);

% correct aerosol radius for water, cm
aRp =
rpdry.*((Imass./inorgdensity+org./OADensity+water./waterdensity)./(Imass./inorgdensity+
org./OADensity))^(1.0/3.0);

```

```

lcoat(i)=0.1*aRp; %coating thickness

% Calculate diagnostic ratio 3*V/(S*rp), units: length/length
threeVdivSrp(i) = 3.0.*awL./(aSa.*aRp);

% Diffusivity for coating (Dcoat)

%Dcoat=1e-12

%if aRH<0.7                % Default cutoff at 70%, new cutoff with Surratt
group coating data at 80%

    if aRH<0.8

        %   Dcoat = exp(6.55*aRH-34.488);   % Derived from Zhang et al 2015 base on
alpha-pinene oxidation products coating.

            Dcoat = 2E-11*exp(12.901*aRH);    % Fitted curve from Surratt lab a-pinene
coating experiment (2017)

        else

            Dcoat = 1e-5; % CMAQ default coating diffusivity cm^2/s

        end

        %Dcoat=10^(7.18*aRH-12.7);          % Pye 2017 coat diffusivity calculation without
cutoff point

    for tduration = 1:6

        [runsuccess,iepoxsout,tetrolout,betaout,gmaout,kpout] = cmaq_uptake(i, awL,
aHplusActivity, ay072, ay073, ...

```

```
awaterconc, aLEP, aSa, aT, aRH, apH, aNH4, aRp,  
tduration,Dcoat,lcoat);
```

```
iepoxos(i,tduration)= iepoxosout;
```

```
tetrol(i,tduration) = tetrolout;
```

```
totsoa(i,tduration) = tetrolout+iepoxosout;
```

```
beta(i)=betaout; % beta will be the same for all tduration, just save last one
```

```
kparticle(i)=kpout; % kp will be the same for all tduration, just save last one
```

```
iepox(i)=aLEP;
```

```
gma(i)=gmaout;
```

```
savenewawL(i) = awL; % save new awL for this line to array
```

```
savenewLWC(i) = awaterconc; % save new awaterconc
```

```
savenewSA(i) = aSa; % save new aSa
```

```
savenewHplus(i) = aHplusActivity; % save new aHplusActivity
```

```
pH(i) = apH; % save apH
```

```
Dorg(i)=Dcoat; % save coating diffusion coefficient
```

```
% Diagnostic info
```

```
if ( runsuccess)
```

```
    fprintf('Row completed: %d\n', i);
```

```
else
```

```
    fprintf('Row did not complete, STOP AND DEBUG!!!!!!!!!!!! %d\n', i);
```

```

        fprintf('Hour did not complete, STOP AND DEBUG!!!!!!!!!! %d\n', i);
    end;

    runsuccess = false;

end;

end;

SOAtotal = iepoxos(:,6)+tetrol(:,6);
%SOAtotal = iepoxos(:,60)+tetrol(:,60);

%% diagnostic information
%datapts = linspace(1,m,m);
%
%plot( datapts, iepoxos(:,12))
%%plot( datapts, iepoxos(:,60))
%
%title('IEPOXOS CMAQ-box')
%saveas( gcf, 'iepoxos.cmaq3.png')
%
%plot( datapts, tetrol(:,12))
%%plot( datapts, tetrol(:,60))
%
```

```

%title('Tetrol CMAQ-box')

%saveas( gcf, 'tetrol.cmaq3.png')

%

%plot( datapts, SOAtotal)

%title('SOA total CMAQ-box')

%saveas( gcf, 'soatotal.cmaq3.png')

%

%plot( datapts, beta(:))

%title('Beta CMAQ-box')

%saveas( gcf, 'beta.cmaq3.png')

% determine mean and standard deviation of beta

mean(beta)

std(beta)

% exit

fileID = fopen('cmaq_base.txt','w');

fprintf(fileID,'%12s %12s %12s %12s %12s %12s %12s\n',

'line','hour','soa','kp','Dorg','lcoat','gamma');

aiepox=0;

for line = 1:m;

for tduration = 1:6

```

```
fprintf(fileID,'%12d %12d %12.6e %12.6e %12.6e %12.6e %12.6e\n', line, tduration,
totsoa(line,tduration),kparticle(line),Dorg(line),lcoat(line),gma(line));

end;

end;
```

cmaq_uptake.m

```
% CMAQ uptake algorithms. Box model originally from
% Simplified Gas-Aerosol Model for Mechanism Analysis ~ simpleGAMMA.m
%%%%%%%%%%%%%%%%%%%%%%%%%%%%%%%%%%%%%%%%%%%%%%%%%%%%%%%%%%%%%%%%%%%%%%%%
%%%%%%%%%
% 9/8/14 HOTP (CMAQ v1)
% Modified to compute uptake following CMAQ algorithms. Extraneous information
removed for clarity.
%
%%%%%%%%%%%%%%%%%%%%%%%%%%%%%%%%%%%%%%%%%%%%%%%%%%%%%%%%%%%%%%%%%%%%%%%%
%%%%%%%%%
% 9/10/14 SHB
% Modified to save data every hour for each input line
%
%%%%%%%%%%%%%%%%%%%%%%%%%%%%%%%%%%%%%%%%%%%%%%%%%%%%%%%%%%%%%%%%%%%%%%%%
%%%%%%%%%
% 9/11/14 SHB (CMAQ v1.1)
% Modified
```

% H_iejox from 3e7 (original simpleGAMMA) to 2.7e6 (Pye et al. 2013)

% k_H+_tetrol from 9e-4 M2/s to 2e-4 M2/s

% k_H+_iejoxos = 2e-4 * (5.2e-1/5.3e-2) = 2e-3 %% Piletic et al. (2013)

% k_HSO4-_iejoxos = 2.9e-6 * (5.2e-1/5.3e-2) = 2.8453e-05 %% Piletic et al. (2013)

%

%%

%%

% 9/17/14 SHB (CMAQ v2)

% Added 3.1e-7*NH4 into kp calculations

%

%%

%%

% 9/29/14 SHB (CMAQ v3)

% Changed the data input (SOAS_LRK_v3).

% Used LRK ambient inorganic loading (ACSM SO4+NH4+NO3) to calculate awL.

%

%%

%%

% 9/30/14 SHB (CMAQ v4)

% Replaced [waterconc] with 55.5 M

%%

% August 2015 HOTP

% Modified to include IEPOX conc calculation, similar kp formula for both CMAQ and simpleGAMMA,

% and BETA calculation for simpleGAMMA

%%%%%%%%%

% 8/27/15 SHB

% Added kp in function to get kp values

%%%%%%%%%

% 8/2016 HOTP

% Cleanup and added Riedel 2016 rate constants

%%%%%%%%%

% 8/2016

% Add gma, kp in function

%%%%%%%%%

% 5/2017 MM

% Add diffusivity resistor in gma (Gaston 2014), add coating diffusivity Dcoat (Zhang 2015)

%%%%%%%%%

% 7/2017 MM

% Change lcoat=0.1*rp to lcoat=0.3*rp

% 9/2017 MM

% Change lcoat back to 0.1*rp

```

%
=====

=====

% clear;

function [runsuccess,iepozos,tetrol,beta,gma,kp] = cmaq_uptake(i, awL, aHplusActivity,
ay072, ay073, awaterconc, aIEP, aSa, aT, aRH, apH, aNH4, aRp, tduration,Dcoat,lcoat)

%tic;

runsuccess = false;

disp('Running CMAQ uptake, low-NOx mode.');
```

% Species Glossary. See McNeill 2012 Supplemental Information for full names.

```

names{07} = '[IEPOX] (gas)';
names{72} = '[BISULFATE] (aq)';
names{73} = '[SULFATE] (aq)';
names{76} = '[IEPOXOS] (aq)';
names{77} = '[tetrol] (aq)';
```

%%% Declaration of concentration, emission, and deposition vectors.

```

y = zeros(78,1);
y0 = zeros(78,1);
```

```

E = zeros(78,1);
d = zeros(78,1);

% Initialization

options = odeset;

% Time Definition (incorporated from original initialization file.). Set duration to 12 hours
duration = tduration;
tspan = [0 duration*3600]; %tduration for hours running time
%tspan = [0 duration*60]; %tduration for minutes running time
%tspan = [0 duration*1]; %tduration for seconds running time

% Define initial simulation parameters.

% Values from input file passed from driver
wL      = awL;
HplusActivity = aHplusActivity;
y0(72)  = ay072;
y0(73)  = ay073;
waterconc = awaterconc;
y0(7)   = aIEP;
Sa      = aSa;
T       = aT;

```

RH = aRH;

pH = apH;

Hplus = 10^{-(pH)};

NH4 = aNH4;

R = aRp; %Radius is estimated from measurement: Rp of max particle num

conc per time

Dcoat = Dcoat; %Dcoat=Dorg

lcoat = lcoat;

% Radius from Whitby (used to be in remote_start)

%R = 148.5e-7; % Surface area averaged sulfate particle radius in (cm, Whitby 1978

Table 4)

% Henry's Law constant	Species	Source
H(1) = 3e7;	% IEPOX	Nguyen et al.
ACP 2014.		
%H(1) = 2.7e6;	% IEPOX	Pye et al.
(2013)		
%H(1) = 3e8;	% IEPOX	Kampf et
al. ES&T 2013, Waxman et al. ES&T 2015.		
%H(1) = 8e7; %optimal run		

% Molecular Masses (for kmt)

Species

Source

M(1) = 0.118077;

% IEPOX

% Accomodation Coefficient

Species

Source

alpha(1) = 0.02;

% IEPOX

params = [wL]; %, CH4, CO2];

w = (8*8.314*T./3.1415/M).^0.5*100; % Thermal Velocity vector, cm/s.

Dg = 1.9*M^(-2/3); % Estimated Gas-phase Diffusion Coefficient, cm2/s.

(Schnoor 1996, via Lim)

% Particle-phase reaction rate constant for tetrol formation

ktetrol = 9e-4; % 1/M2 1/s, Eddingsaas 2010 JPhysChemA

%ktetrol = 3.4e-4; % 1/M2 1/s, Riedel 2016 ACP

% Particle-phase reaction rate constant for organosulfate formation

%kos = 8.83e-3; % 1/M2 1/s, value based on Eddingsaas 2010 tetrol and Piletic

2013 PCCP relative value

kos = ktetrol*4.8e-4/3.4e-4; % 1/M2 1/s, value based on Riedel 2016 relative value

% Particle-phase reaction rate constant: pseudo first order

kp = (ktetrol.*HplusActivity.*waterconc)+(1.31e-5.*y0(72).*waterconc)+(3.1e-7.*NH4.*waterconc) ...

+(kos.*HplusActivity.*y0(73)); % Particle-phase rate constant.

Eq.4 (Pye 2013), this work

% Ratio of OS to OS+tetrol

beta = kos.*HplusActivity*y0(73)/kp;

% diffusio-reactive parameter

q = R*sqrt(kp./(1e-5)); % Eq.3 (Pye 2013).

Diffusivity in aerosol phase, Da=1e-5 cm²/s (1e-9 m²/s)

fq = coth(q)-(1./q); % Eq.2 (Pye 2013)

% coating thickness

%lcoat = 0.1*R; % estimated

%lcoat = 0.3*R; % base on Surratt lab

experiment data

% % Diffusivity for coating (Dcoat)

% %Dcoat=1e-12

% if RH<0.7

% Dcoat = exp(0.0655*RH*100-34.488); % Derived from Zhang et al 2015 base on alpha-pinene oxidation products coating.

```

% else

%     Dcoat = 1e-5; % CMAQ default coating diffusivity cm^2/s

% end

% Gamma (gma) and khet (kh)

th = 0; %for base case

%th = w.*0.1*R.*R./(0.9*R.*4*(0.3)*82.06*(1e-3)*T.*Dcoat); % third term in gamma
equation

%gma = ((1/alpha)+(w./(4*H*(1e-3)*82.06*T.*sqrt(kp.*(1e-5))).*1./fq)).^(-1); %
Uptake coefficient. Eq.1 (Pye 2013) default case

gma = ((1/alpha)+(w./(4*H*(1e-3)*82.06*T.*sqrt(kp.*(1e-5))).*1./fq)+th).^(-1); %
Uptake coefficient. Eq.1 (Pye 2013)

%gma = ((1/alpha)+(w./(4*H*(1e-3)*82.06*T.*sqrt(kp.*(1e-5))).*1./fq)+(w.*(5e-
7)*R/((R-(5e-7))*4*(10e-9)*H*82.06*T.*(Dcoat)))).^(-1);

kh = (((R/Dg)+(4./(w.*gma))).^(-1)).*Sa; % Heterogeneous
rate constant. Eq.8 (Jacob 2000). Diffusivity in gas phase Dg=1e-1 cm^2/s (1e-5 m^2/s)

% Declaration and initialization of [datasave], a matrix that compiles all
% [y] and [t] vectors into a single term.

datasave = cat(1,0,y0);

datasave = transpose(datasave);

%%% CMAQ hetchem updated 07/16/2014 by SHB.

[t, P] = ode15s(@cmaq_ode_fun, tspan, y0, options, params, kh, beta);

```

```
% Combine time and the concentration outputs into a single output matrix,  
% [P]. Note that all species indices of [P] are the same as [y]+1 when  
% comparing data between the two.
```

```
data = cat(2,t,P);  
datasave = cat(1,datasave, data);  
clear data;
```

```
% Save the last point in vector [y] as a text file, [y0.txt], to be called  
% for another iteration, if desired.
```

```
y = P(end,:);  
save y0.txt y -ASCII
```

```
%toc
```

```
%%% CMAQ hetchem updated 07/16/2014 by SHB.
```

```
SOAmass = ...  
    datasave(:,76+1).*0.21612+ ...    % IEPOXOS  
    datasave(:,77+1).*0.13612;    % tetrol
```

```
[lastt,other] = size(datasave);
```

```
iepoxtos = (datasave(lastt,76+1).*0.21612)';
```

```

tetrol = (datasave(lastt,77+1).*0.13612)';

disp(['Total generated SOA mass after ',num2str(duration),' hours =
',num2str(SOAmass(end)),' kg / L aerosol.'])

% Plot given species with respect to time.

t_hours = datasave(:,1)/3600; %hours running time
%t_hours = datasave(:,1)/60; %minutes running time
%t_hours = datasave(:,1)/1; %seconds running time

% update status

runsuccess = true;

% End code.

cmaq_ode_fun.m

%
% Simplified GAMMA - Defining ODE Function ~ simpleGAMMAODEfun.m
% Columbia University 2013
%
=====
=====

% Adapted from GAMMAODEfun v.1.1, originally written by VFM.
% Build 1.3c, July 12 2013, updated by JLW.

```

```

%
% Modified to follow CMAQ algorithms with inputs from Look Rock, TN
%
%%%%%%%%%%%%%%%%%%%%%%%%%%%%%%%%%%%%%%%%%%%%%%%%%%%%%%%%%%%%%%%%%%%%%%%%
%%
% 9/17/14 SHB
% Modified to include 3.1e-7*NH4 in tetrol diff eq.
%
%%%%%%%%%%%%%%%%%%%%%%%%%%%%%%%%%%%%%%%%%%%%%%%%%%%%%%%%%%%%%%%%%%%%%%%%
% August 2015 HOTP
% Modified to include IEPOX conc calculation, similar kp formula for both CMAQ and
simpleGAMMA,
% and BETA calculation for simpleGAMMA
% 8/2016 HOTP
% Cleaned up unused and added beta
%
=====
=====

function dy = cmaq_ode_fun(t, y, params, kh, beta)

% set all differential equations to zero for initialization (IEPOX dy remains zero)
dy = zeros(78,1);

```

```
% get parameters out of vector 'params'.
```

```
wL = params(1);
```

```
% IEPOXOS formation
```

```
dy(76) = (beta.*kh.*(y(7).*1e3./(wL.*6.022e23)));
```

```
% Tetrol formation
```

```
dy(77) = (1-beta).*kh.*(y(7).*1e3./(wL.*6.022e23));
```

```
iepox_fun.m
```

```
% returns IEPOX concentration based on hour of day and CIMS sensitivity to IEPOX  
and ISOPOOH
```

```
function[ iepoxmolcm3 ] = iepox_fun( origiepoxmolcm3, datetimeedt )
```

```
% function inputs:
```

```
% origiepoxmolcm3 is iepox in mol/cm3 (total IEPOX + ISOPOOH signal)
```

```
% datetimeedt is date/time edt expressed as days since Jan 1, 1900 (Igor convention)
```

```
% m/z 177 sensitivities (Budisulistiorini et al. 2015)
```

```
SIEPOX = 10e-7; % signal/ppt
```

```
SISOPOOH = 9.9e-8; % signal/ppt
```

```
% determine hour of day
hour = floor( (datetimedt - floor(datetimedt))*24 );

% find ISOPOOH:IEPOX factor from CMAQ as a function of hour EDT (GMT-4)
if ( hour == 1 )
    alpha = 0.28;
elseif ( hour == 2 )
    alpha = 0.28;
elseif ( hour == 3 )
    alpha = 0.29;
elseif ( hour == 4 )
    alpha = 0.30;
elseif ( hour == 5 )
    alpha = 0.29;
elseif ( hour == 6 )
    alpha = 0.26;
elseif ( hour == 7 )
    alpha = 0.27;
elseif ( hour == 8 )
    alpha = 0.34;
elseif ( hour == 9 )
    alpha = 0.43;
elseif ( hour == 10 )
```

```
alpha = 0.55;
elseif ( hour == 11 )
    alpha = 0.66;
elseif ( hour == 12 )
    alpha = 0.71;
elseif ( hour == 13 )
    alpha = 0.70;
elseif ( hour == 14 )
    alpha = 0.66;
elseif ( hour == 15 )
    alpha = 0.61;
elseif ( hour == 16 )
    alpha = 0.54;
elseif ( hour == 17 )
    alpha = 0.54;
elseif ( hour == 18 )
    alpha = 0.59;
elseif ( hour == 19 )
    alpha = 0.65;
elseif ( hour == 20 )
    alpha = 0.65;
elseif ( hour == 21 )
    alpha = 0.56;
```

```
elseif ( hour == 22 )
```

```
    alpha = 0.46;
```

```
elseif ( hour == 23 )
```

```
    alpha = 0.36;
```

```
elseif ( hour == 0 )
```

```
    alpha = 0.29;
```

```
end
```

```
% value to return
```

```
%iepoxmolcm3 = origiepoxmolcm3 / ( SIEPOX + alpha * SISOPOOH )
```

```
iepoxmolcm3 = origiepoxmolcm3 / ( 1.0 + alpha );
```

REFERENCES

1. Janssen, N. A.; Hoek, G.; Simic-Lawson, M.; Fischer, P.; van Bree, L.; ten Brink, H.; Keuken, M.; Atkinson, R. W.; Anderson, H. R.; Brunekreef, B.; Cassee, F. R., Black carbon as an additional indicator of the adverse health effects of airborne particles compared with PM10 and PM2.5. *Environmental health perspectives* **2011**, *119*, (12), 1691-9.
2. Zhang, Q.; Jimenez, J. L.; Canagaratna, M. R.; Allan, J. D.; Coe, H.; Ulbrich, I.; Alfarra, M. R.; Takami, A.; Sun, Y. L.; Dzepina, K.; Dunlea, E.; Docherty, K.; DeCarlo, P. F.; Salcedo, D.; Onasch, T.; Jayne, J. T.; Miyoshi, T.; Shimojo, A.; Hatakeyama, S.; Takegawa, N.; Kondo, Y.; Schneider, J.; Drewnick, F.; Borrmann, S.; Weimer, S.; Demerjian, K.; Williams, P.; Bower, K.; Bahreini, R.; Cottrell, L.; Griffin, R. J.; Rautiainen, J.; Sun, J. Y.; Zhang, Y. M.; Worsnop, D. R., Ubiquity and dominance of oxygenated species in organic aerosols in anthropogenically - influenced Northern Hemisphere midlatitudes. *Geophysical Research Letters* **2007**, *34*, (13).
3. Kiendler-Scharr, A.; Wildt, J.; Dal Maso, M.; Hohaus, T.; Kleist, E.; Mentel, T. F.; Tillmann, R.; Uerlings, R.; Schurr, U.; Wahner, A., New particle formation in forests inhibited by isoprene emissions. *Nature* **2009**, *461*, (7262), 381-4.
4. Liao, J.; Froyd, K. D.; Murphy, D. M.; Keutsch, F. N.; Yu, G.; Wennberg, P. O.; St Clair, J. M.; Crouse, J. D.; Wisthaler, A.; Mikoviny, T.; Jimenez, J. L.; Campuzano-Jost, P.; Day, D. A.; Hu, W.; Ryerson, T. B.; Pollack, I. B.; Peischl, J.; Anderson, B. E.; Ziemba, L. D.; Blake, D. R.; Meinardi, S.; Diskin, G., Airborne measurements of organosulfates over the continental U.S. *J Geophys Res Atmos* **2015**, *120*, (7), 2990-3005.
5. Guenther, A.; Karl, T.; Harley, P.; Wiedinmyer, C.; Palmer, P. I.; Geron, C., Estimates of global terrestrial isoprene emissions using MEGAN (Model of Emissions of Gases and Aerosols from Nature). *Atmospheric Chemistry and Physics* **2006**, *6*, (11), 3181-3210.
6. Surratt, J. D.; Chan, A. W.; Eddingsaas, N. C.; Chan, M.; Loza, C. L.; Kwan, A. J.; Hersey, S. P.; Flagan, R. C.; Wennberg, P. O.; Seinfeld, J. H., Reactive intermediates revealed in secondary organic aerosol formation from isoprene. *Proc Natl Acad Sci U S A* **2010**, *107*, (15), 6640-5.
7. Nguyen, T. B.; Crouse, J. D.; Teng, A. P.; St Clair, J. M.; Paulot, F.; Wolfe, G. M.; Wennberg, P. O., Rapid deposition of oxidized biogenic compounds to a temperate forest. *Proc Natl Acad Sci U S A* **2015**, *112*, (5), E392-401.
8. Krechmer, J. E.; Coggon, M. M.; Massoli, P.; Nguyen, T. B.; Crouse, J. D.; Hu, W.; Day, D. A.; Tyndall, G. S.; Henze, D. K.; Rivera-Rios, J. C.; Nowak, J. B.; Kimmel, J. R.; Mauldin, R. L., 3rd; Stark, H.; Jayne, J. T.; Sipila, M.; Junninen, H.; Clair, J. M.; Zhang, X.; Feiner, P. A.; Zhang, L.; Miller, D. O.; Brune, W. H.; Keutsch, F. N.; Wennberg, P. O.; Seinfeld, J. H.; Worsnop, D. R.; Jimenez, J. L.; Canagaratna, M. R., Formation of Low Volatility Organic Compounds and Secondary Organic Aerosol from Isoprene Hydroxyhydroperoxide Low-NO Oxidation. *Environ Sci Technol* **2015**, *49*, (17), 10330-9.
9. Paulot, F.; Crouse, J. D.; Kjaergaard, H. G.; Kurten, A.; St Clair, J. M.; Seinfeld, J. H.; Wennberg, P. O., Unexpected epoxide formation in the gas-phase photooxidation of isoprene. *Science (New York, N.Y.)* **2009**, *325*, (5941), 730-3.

10. Zhang, H.; Surratt, J. D.; Lin, Y. H.; Bapat, J.; Kamens, R. M., Effect of relative humidity on SOA formation from isoprene/NO photooxidation: enhancement of 2-methylglyceric acid and its corresponding oligoesters under dry conditions. *Atmospheric Chemistry and Physics* **2011**, *11*, (13), 6411-6424.
11. Lin, Y. H.; Zhang, Z.; Docherty, K. S.; Zhang, H.; Budisulistiorini, S. H.; Rubitschun, C. L.; Shaw, S. L.; Knipping, E. M.; Edgerton, E. S.; Kleindienst, T. E.; Gold, A.; Surratt, J. D., Isoprene epoxydiols as precursors to secondary organic aerosol formation: acid-catalyzed reactive uptake studies with authentic compounds. *Environ Sci Technol* **2012**, *46*, (1), 250-8.
12. Lin, Y. H.; Zhang, H.; Pye, H. O.; Zhang, Z.; Marth, W. J.; Park, S.; Arashiro, M.; Cui, T.; Budisulistiorini, S. H.; Sexton, K. G.; Vizuete, W.; Xie, Y.; Luecken, D. J.; Piletic, I. R.; Edney, E. O.; Bartolotti, L. J.; Gold, A.; Surratt, J. D., Epoxide as a precursor to secondary organic aerosol formation from isoprene photooxidation in the presence of nitrogen oxides. *Proc Natl Acad Sci U S A* **2013**, *110*, (17), 6718-23.
13. Lin, Y. H.; Sexton, K. G.; Jaspers, I.; Li, Y. R.; Surratt, J. D.; Vizuete, W., Application of chemical vapor generation systems to deliver constant gas concentrations for in vitro exposure to volatile organic compounds. *Environ Sci Process Impacts* **2014**, *16*, (12), 2703-10.
14. Nguyen, T. B.; Coggon, M. M.; Bates, K. H.; Zhang, X.; Schwantes, R. H.; Schilling, K. A.; Loza, C. L.; Flagan, R. C.; Wennberg, P. O.; Seinfeld, J. H., Organic aerosol formation from the reactive uptake of isoprene epoxydiols (IEPOX) onto non-acidified inorganic seeds. *Atmospheric Chemistry and Physics* **2014**, *14*, (7), 3497-3510.
15. Jacobs, M. I.; Burke, W. J.; Elrod, M. J., Kinetics of the reactions of isoprene-derived hydroxynitrates: gas phase epoxide formation and solution phase hydrolysis. *Atmospheric Chemistry and Physics* **2014**, *14*, (17), 8933-8946.
16. Budisulistiorini, S. H.; Li, X.; Bairai, S. T.; Renfro, J.; Liu, Y.; Liu, Y. J.; McKinney, K. A.; Martin, S. T.; McNeill, V. F.; Pye, H. O. T.; Nenes, A.; Neff, M. E.; Stone, E. A.; Mueller, S.; Knote, C.; Shaw, S. L.; Zhang, Z.; Gold, A.; Surratt, J. D., Examining the effects of anthropogenic emissions on isoprene-derived secondary organic aerosol formation during the 2013 Southern Oxidant and Aerosol Study (SOAS) at the Look Rock, Tennessee ground site. *Atmospheric Chemistry and Physics* **2015**, *15*, (15), 8871-8888.
17. Rattanavaraha, W.; Chu, K.; Budisulistiorini, S. H.; Riva, M.; Lin, Y.-H.; Edgerton, E. S.; Baumann, K.; Shaw, S. L.; Guo, H.; King, L.; Weber, R. J.; Neff, M. E.; Stone, E. A.; Offenberg, J. H.; Zhang, Z.; Gold, A.; Surratt, J. D., Assessing the impact of anthropogenic pollution on isoprene-derived secondary organic aerosol formation in PM_{2.5} collected from the Birmingham, Alabama, ground site during the 2013 Southern Oxidant and Aerosol Study. *Atmospheric Chemistry and Physics* **2016**, *16*, (8), 4897-4914.
18. Pye, H. O.; Pinder, R. W.; Piletic, I. R.; Xie, Y.; Capps, S. L.; Lin, Y. H.; Surratt, J. D.; Zhang, Z.; Gold, A.; Luecken, D. J.; Hutzell, W. T.; Jaoui, M.; Offenberg, J. H.; Kleindienst, T. E.; Lewandowski, M.; Edney, E. O., Epoxide pathways improve model predictions of isoprene markers and reveal key role of acidity in aerosol formation. *Environ Sci Technol* **2013**, *47*, (19), 11056-64.
19. Pye, H. O. T.; Murphy, B. N.; Xu, L.; Ng, N. L.; Carlton, A. G.; Guo, H. Y.; Weber, R.; Vasilakos, P.; Appel, K. W.; Budisulistiorini, S. H.; Surratt, J. D.; Nenes, A.; Hu, W. W.; Jimenez, J. L.; Isaacman-

- VanWertz, G.; Misztal, P. K.; Goldstein, A. H., On the implications of aerosol liquid water and phase separation for organic aerosol mass. *Atmospheric Chemistry and Physics* **2017**, *17*, (1), 343-369.
20. Budisulistiorini, S. H.; Nenes, A.; Carlton, A. G.; Surratt, J. D.; McNeill, V. F.; Pye, H. O. T., Simulating Aqueous-Phase Isoprene-Epoxydiol (IEPOX) Secondary Organic Aerosol Production During the 2013 Southern Oxidant and Aerosol Study (SOAS). *Environ Sci Technol* **2017**, *51*, (9), 5026-5034.
21. Riva, M.; Bell, D. M.; Hansen, A. M.; Drozd, G. T.; Zhang, Z.; Gold, A.; Imre, D.; Surratt, J. D.; Glasius, M.; Zelenyuk, A., Effect of Organic Coatings, Humidity and Aerosol Acidity on Multiphase Chemistry of Isoprene Epoxydiols. *Environ Sci Technol* **2016**, *50*, (11), 5580-8.
22. Claeys, M.; Graham, B.; Vas, G.; Wang, W.; Vermeylen, R.; Pashynska, V.; Cafmeyer, J.; Guyon, P.; Andreae, M. O.; Artaxo, P.; Maenhaut, W., Formation of secondary organic aerosols through photooxidation of isoprene. *Science (New York, N.Y.)* **2004**, *303*, (5661), 1173-6.
23. Edney, E. O.; Kleindienst, T. E.; Jaoui, M.; Lewandowski, M.; Offenberg, J. H.; Wang, W.; Claeys, M., Formation of 2-methyl tetrols and 2-methylglyceric acid in secondary organic aerosol from laboratory irradiated isoprene/NOX/SO2/air mixtures and their detection in ambient PM2.5 samples collected in the eastern United States. *Atmospheric Environment* **2005**, *39*, (29), 5281-5289.
24. Jesse H. Kroll; Nga L. Ng; Shane M. Murphy; Richard C. Flagan, a.; Seinfeld*, J. H., Secondary Organic Aerosol Formation from Isoprene Photooxidation. **2006**.
25. Liu, Y.; Kuwata, M.; Strick, B. F.; Geiger, F. M.; Thomson, R. J.; McKinney, K. A.; Martin, S. T., Uptake of epoxydiol isomers accounts for half of the particle-phase material produced from isoprene photooxidation via the HO2 pathway. *Environ Sci Technol* **2015**, *49*, (1), 250-8.
26. Jason D. Surratt; Shane M. Murphy; Jesse H. Kroll; Nga L. Ng; Lea Hildebrandt; Armin Sorooshian; Rafal Szmigielski; Reinhilde Vermeylen; Willy Maenhaut; Magda Claeys; Richard C. Flagan, a.; John H. Seinfeld*, Chemical Composition of Secondary Organic Aerosol Formed from the Photooxidation of Isoprene. **2006**.
27. St Clair, J. M.; Rivera-Rios, J. C.; Crouse, J. D.; Knap, H. C.; Bates, K. H.; Teng, A. P.; Jorgensen, S.; Kjaergaard, H. G.; Keutsch, F. N.; Wennberg, P. O., Kinetics and Products of the Reaction of the First-Generation Isoprene Hydroxy Hydroperoxide (ISOPOOH) with OH. *J Phys Chem A* **2016**, *120*, (9), 1441-51.
28. Xie, Y.; Paulot, F.; Carter, W. P. L.; Nolte, C. G.; Luecken, D. J.; Hutzell, W. T.; Wennberg, P. O.; Cohen, R. C.; Pinder, R. W., Understanding the impact of recent advances in isoprene photooxidation on simulations of regional air quality. *Atmospheric Chemistry and Physics* **2013**, *13*, (16), 8439-8455.
29. Chen, Y. Z.; Sexton, K. G.; Jerry, R. E.; Surratt, J. D.; Vizuete, W., Assessment of SAPRC07 with updated isoprene chemistry against outdoor chamber experiments. *Atmospheric Environment* **2015**, *105*, 109-120.
30. Odum, J. R.; Hoffmann, T.; Bowman, F.; Collins, D.; Flagan, R. C.; Seinfeld, J. H., Gas/particle partitioning and secondary organic aerosol yields. *Environmental Science & Technology* **1996**, *30*, (8), 2580-2585.

31. Zhang, Y.; Sanchez, M. S.; Douet, C.; Wang, Y.; Bateman, A. P.; Gong, Z.; Kuwata, M.; Renbaum-Wolff, L.; Sato, B. B.; Liu, P. F.; Bertram, A. K.; Geiger, F. M.; Martin, S. T., Changing shapes and implied viscosities of suspended submicron particles. *Atmospheric Chemistry and Physics* **2015**, *15*, (14), 7819-7829.
32. Lindsay, S. M., *Introduction to nanoscience*. Oxford University Press: Oxford, 2010.
33. Gaston, C. J.; Thornton, J. A.; Ng, N. L., Reactive uptake of N₂O₅ to internally mixed inorganic and organic particles: the role of organic carbon oxidation state and inferred organic phase separations. *Atmospheric Chemistry and Physics* **2014**, *14*, (11), 5693-5707.
34. Song, M.; Marcolli, C.; Zuend, A.; Peter, T., Liquid - liquid phase separation in aerosol particles: Dependence on O:C, organic functionalities, and compositional complexity. *Geophysical Research Letters* **2012**, *39*, (19).
35. Zhang, Y.; Chen, Y.; Lambe, A. T.; Olson, N. E.; Lei, Z.; Craig, R. L.; Zhang, Z.; Gold, A.; Onasch, T.; Jayne, J. T.; Worsnop, D. R.; Gaston, C. J.; Thornton, J. A.; Vizuete, W.; Ault, A. P.; Surratt, J. D., Effect of Aerosol-Phase State on Secondary Organic Aerosol Formation from the Reactive Uptake of Isoprene-Derived Epoxydiols (IEPOX). *Environmental Science & Technology Letters* **2017**, *In review*.
36. Hanson, D. R.; Ravishankara, A. R.; Solomon, S., Heterogeneous Reactions in Sulfuric-Acid Aerosols - a Framework for Model-Calculations. *J Geophys Res-Atmos* **1994**, *99*, (D2), 3615-3629.
37. Schnoor, J. L., *Environmental Modeling: Fate and Transport of Pollutants in Water, Air and Soil*. Wiley: 1996; p 4.
38. Song, M.; Marcolli, C.; Krieger, U. K.; Zuend, A.; Peter, T., Liquid-liquid phase separation and morphology of internally mixed dicarboxylic acids/ammonium sulfate/water particles. *Atmospheric Chemistry and Physics* **2012**, *12*, (5), 2691-2712.
39. Anttila, T.; Kiendler-Scharr, A.; Tillmann, R.; Mentel, T. F., On the reactive uptake of gaseous compounds by organic-coated aqueous aerosols: theoretical analysis and application to the heterogeneous hydrolysis of N₂O₅. *J Phys Chem A* **2006**, *110*, (35), 10435-43.
40. Gaston, C. J.; Riedel, T. P.; Zhang, Z.; Gold, A.; Surratt, J. D.; Thornton, J. A., Reactive uptake of an isoprene-derived epoxydiol to submicron aerosol particles. *Environ Sci Technol* **2014**, *48*, (19), 11178-86.
41. Serway, R. A. a. F. J. S. a. V. C., *College physics*. 2009; p 24.
42. Song, M.; Liu, P. F.; Hanna, S. J.; Li, Y. J.; Martin, S. T.; Bertram, A. K., Relative humidity-dependent viscosities of isoprene-derived secondary organic material and atmospheric implications for isoprene-dominant forests. *Atmospheric Chemistry and Physics* **2015**, *15*, (9), 5145-5159.
43. Renbaum-Wolff, L.; Grayson, J. W.; Bateman, A. P.; Kuwata, M.; Sellier, M.; Murray, B. J.; Shilling, J. E.; Martin, S. T.; Bertram, A. K., Viscosity of alpha-pinene secondary organic material and implications for particle growth and reactivity. *Proc Natl Acad Sci U S A* **2013**, *110*, (20), 8014-9.

44. Fountoukis, C.; Nenes, A., ISORROPIA II: a computationally efficient thermodynamic equilibrium model for K⁺-Ca²⁺-Mg²⁺-NH₄⁽⁺⁾-Na⁺-SO₄²⁻-NO₃⁻-Cl⁻-H₂O aerosols. *Atmospheric Chemistry and Physics* **2007**, *7*, (17), 4639-4659.
45. Shrestha, M.; Zhang, Y.; Ebben, C. J.; Martin, S. T.; Geiger, F. M., Vibrational sum frequency generation spectroscopy of secondary organic material produced by condensational growth from alpha-pinene ozonolysis. *J Phys Chem A* **2013**, *117*, (35), 8427-36.
46. Riedel, T. P.; Lin, Y.; Budisulistiorini, S. H.; Gaston, C. J.; Thornton, J. A.; Zhang, Z.; Vizuete, W.; Gold, A.; Surratt, J. D., Heterogeneous Reactions of Isoprene-Derived Epoxides: Reaction Probabilities and Molar Secondary Organic Aerosol Yield Estimates. *Environmental Science & Technology Letters* **2015**, *2*, (2), 38-42.
47. Riedel, T. P.; Lin, Y. H.; Zhang, Z.; Chu, K.; Thornton, J. A.; Vizuete, W.; Gold, A.; Surratt, J. D., Constraining condensed-phase formation kinetics of secondary organic aerosol components from isoprene epoxydiols. *Atmospheric Chemistry and Physics* **2016**, *16*, (3), 1245-1254.
48. Pye, H. O.; Luecken, D. J.; Xu, L.; Boyd, C. M.; Ng, N. L.; Baker, K. R.; Ayres, B. R.; Bash, J. O.; Baumann, K.; Carter, W. P.; Edgerton, E.; Fry, J. L.; Hutzell, W. T.; Schwede, D. B.; Shepson, P. B., Modeling the Current and Future Roles of Particulate Organic Nitrates in the Southeastern United States. *Environ Sci Technol* **2015**, *49*, (24), 14195-203.
49. Song, Y. C.; Haddrell, A. E.; Bzdek, B. R.; Reid, J. P.; Bannan, T.; Topping, D. O.; Percival, C.; Cai, C., Measurements and Predictions of Binary Component Aerosol Particle Viscosity. *J Phys Chem A* **2016**.
50. Lopez-Hilfiker, F. D.; Mohr, C.; D'Ambro, E. L.; Lutz, A.; Riedel, T. P.; Gaston, C. J.; Iyer, S.; Zhang, Z.; Gold, A.; Surratt, J. D.; Lee, B. H.; Kurten, T.; Hu, W. W.; Jimenez, J.; Hallquist, M.; Thornton, J. A., Molecular Composition and Volatility of Organic Aerosol in the Southeastern U.S.: Implications for IEPOX Derived SOA. *Environ Sci Technol* **2016**, *50*, (5), 2200-9.
51. Lim, C. Y.; Browne, E. C.; Sugrue, R. A.; Kroll, J. H., Rapid heterogeneous oxidation of organic coatings on submicron aerosols. *Geophysical Research Letters* **2017**, *44*, (6), 2949-2957.